EOS from combined theory, experiment, and observations

Jeremy Holt
Texas A&M University, College Station

*<u>**Collaborators**</u>**:** A. Bhattacharya, C. Drischler, N. Kaiser, **Y. Lim**, D. Pati, R. Stahulak, C. Wellenhofer

National Nuclear Security Administration NP3M muses

INT program: The r-process and the nuclear EOS after LIGO-Virgo's third observing run, 5/23/2021

Neutron stars: a novel window into strongly interacting matter and the nuclear force

- **Radius** (NICER PSR J0030+0451, NICER-XMM PSR J0740+6620)
- **Maximum mass** (PSR J0740+6620)
- **Tidal deformabilities** (GW170817)
- **Moments of inertia** (PSR J0737-3039A)

PSR J0030+0451

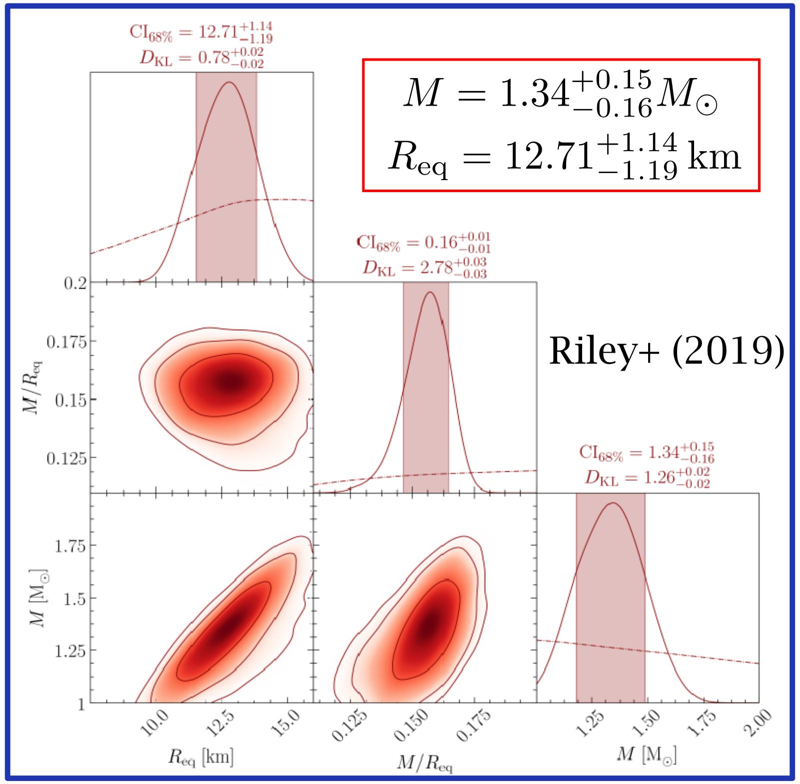

PSR J0740-6620

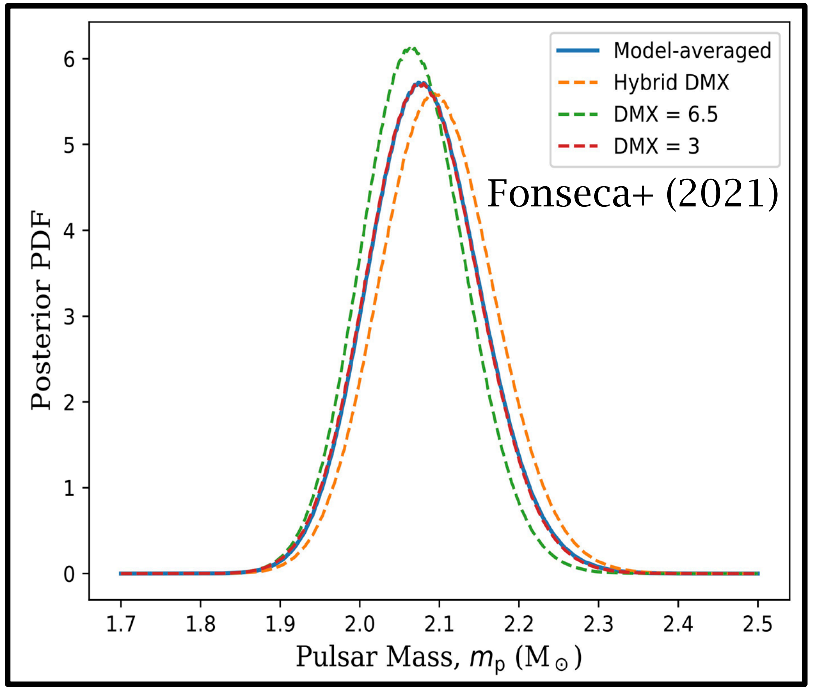

GW170817

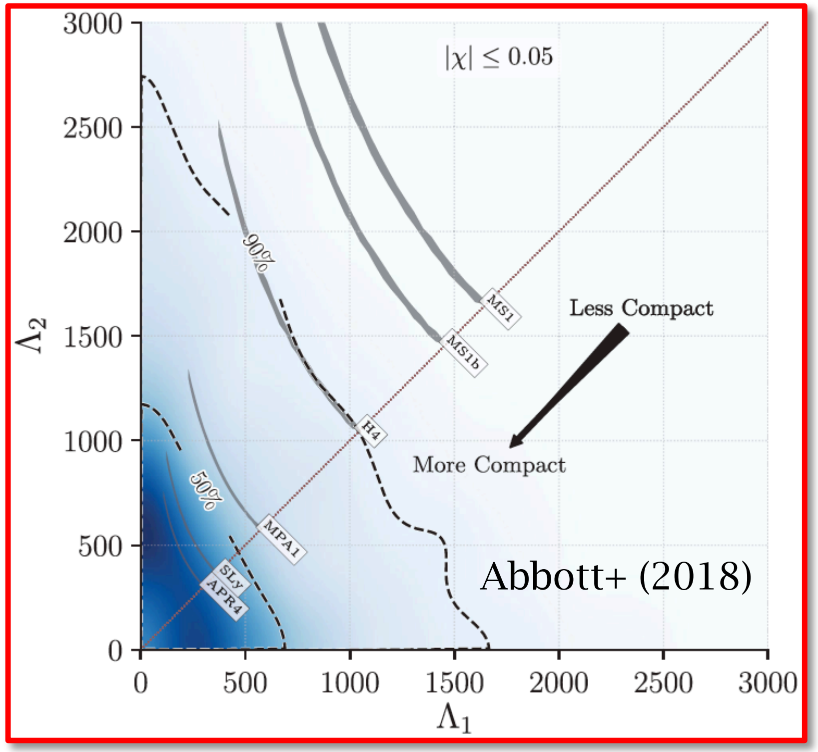

Neutron stars: constraints from nuclear theory and experiment

- **Chiral effective field theory:**
  1. Nuclear forces fitted to few-body systems (^{2}H, ^{3}H, ^{3}He)
  2. Nuclear forces fitted to nuclear many-body systems

  → neutron star matter

  3. Generically leads to **soft equation of state** between 1-2 normal nuclear densities

- **Nuclear experiments on neutron-rich nuclei**
  1. Neutron skin thickness
  2. Electric dipole polarizability
  3. Charge radii of mirror nuclei

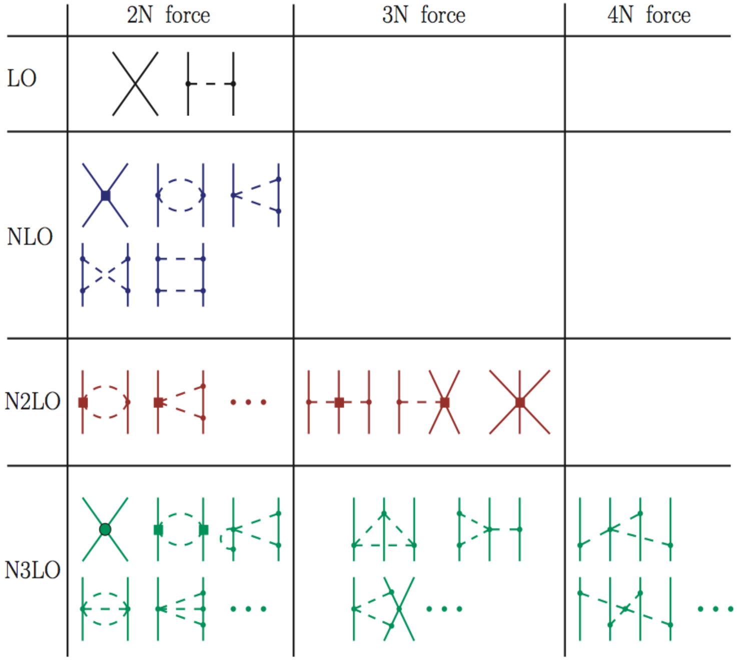

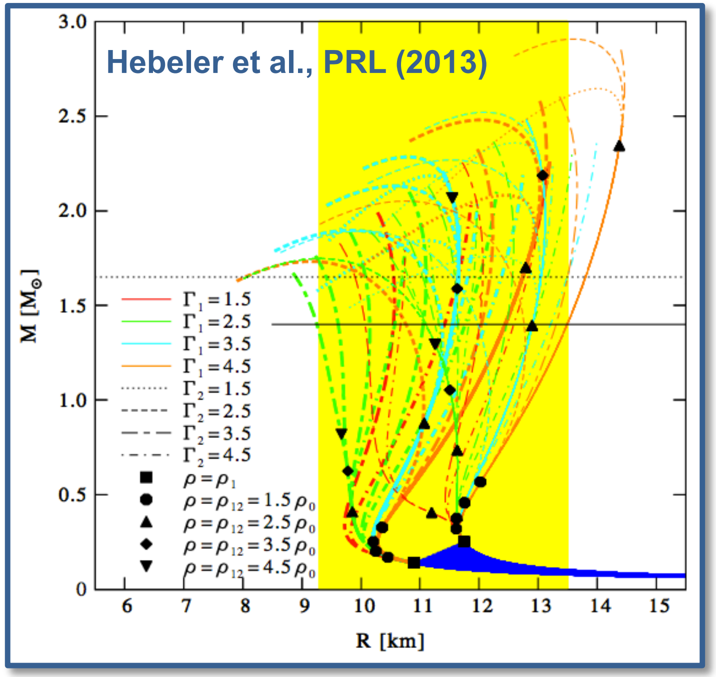

5/2/22 FRIB ribbon cutting

Chiral effective field theory (EFT) for nuclear forces

1. Natural Separation of Scales

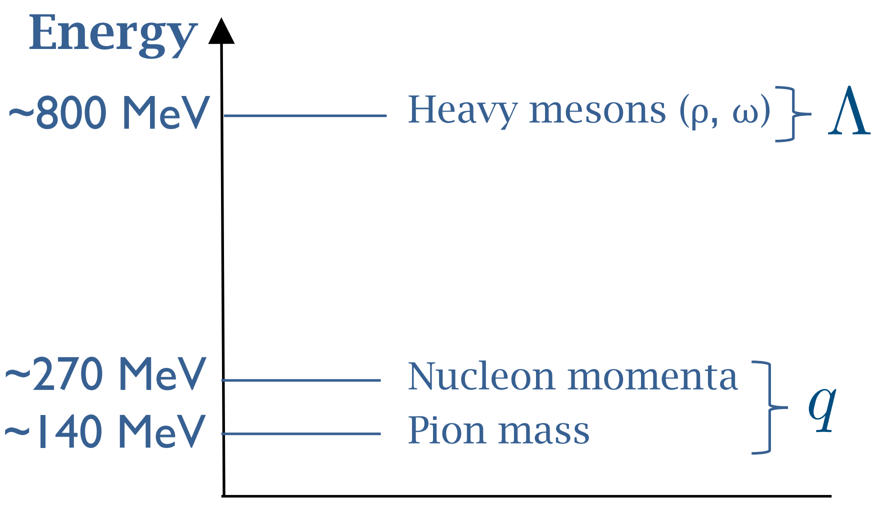

2. Goldstone bosons (pions) weakly-coupled at low momenta

$$\mathcal{L}_{\pi\pi}^{(2)} = \frac{1}{2}\partial_\mu \vec{\pi} \cdot \partial^\mu \vec{\pi} + \frac{1}{2f_\pi^2}(\partial_\mu \vec{\pi} \cdot \vec{\pi})^2$$

$$\mathcal{L}_{\pi N}^{(1)} = \bar{N}\left(i\gamma^\mu D_\mu - m - \frac{g_A}{2f_\pi}\gamma^\mu \gamma_5 \vec{\tau} \cdot \partial_\mu \vec{\pi}\right) N$$

Nuclear forces from chiral EFT

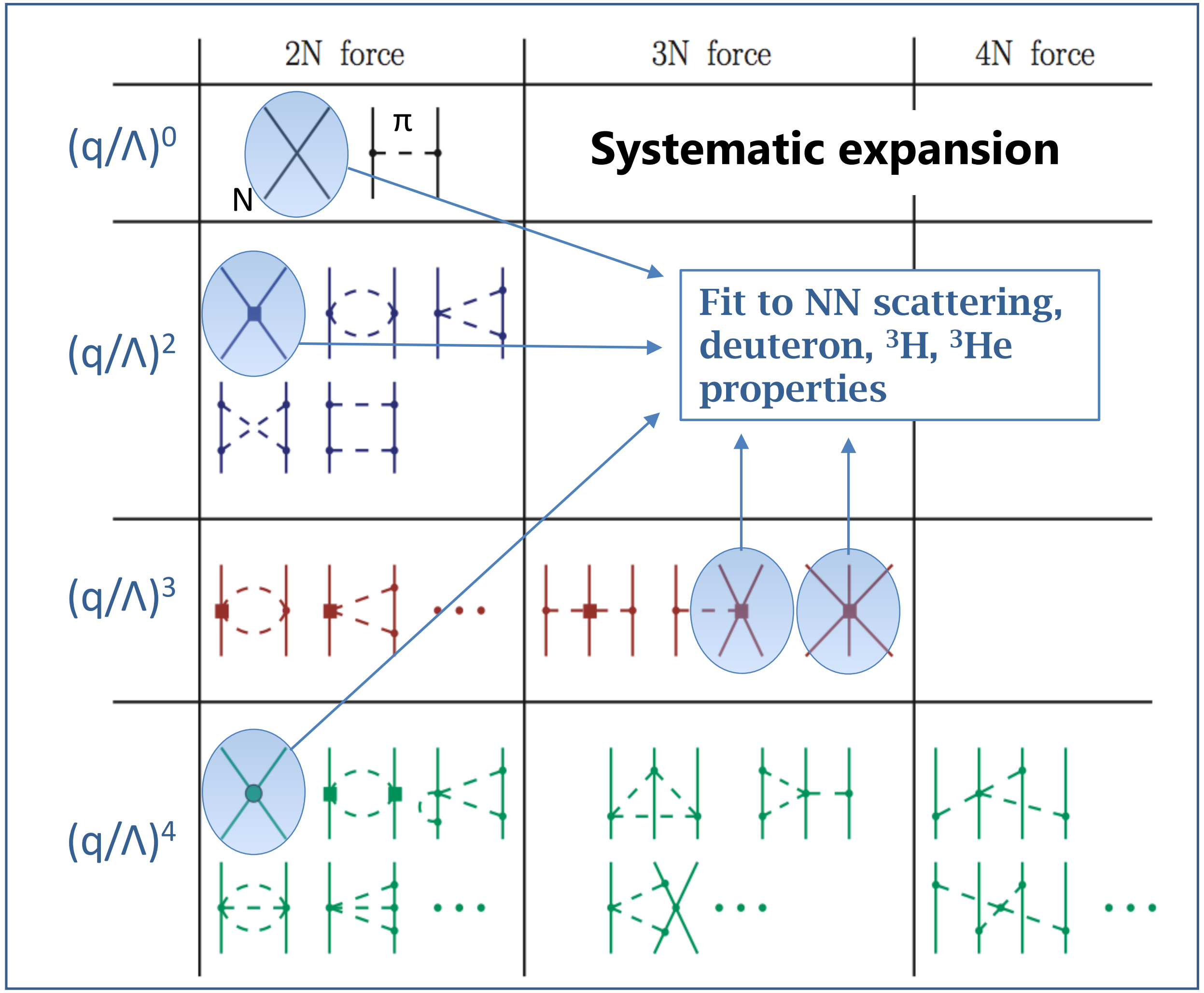

Enables uncertainty quantification

Steady progress and refinements in chiral nuclear forces

- (2003) Entem & Machleidt: 4th-order NN force, *PRC* (2003)
- (2013) Ekström, Baardsen, Forssén,…: optimized NN force at 3rd-order, *PRL* (2013)
- (2014) Gezerlis, Tews, Epelbaum, …: Local NN force at 3rd-order for QMC, *PRC* (2014)
- (2015) Epelbaum, Krebs, and Meissner: improved NN force at 4th-order, *EPJA* (2015)
- (2015) Epelbaum, Krebs, and Meissner: NN forces at 5th-order, *PRL* (2015)
- (2015) Ekström, Jansen, Wendt,…: NN force at 3rd-order fitted to medium-mass nuclei, *PRC* (2015)
- (2015) Piarulli, Girlanda,…: Minimally nonlocal NN force at 4th-order with Δ isobars, *PRC* (2015)
- (2017) Entem, Machleidt, Nosyk: NN force at 5th-order, *PRC* (2017)
- (2018) Reinert, Krebs, Epelbaum: Semi-local NN force at 5th-order, *EPJA* (2018)
- (2018) Ekström, Hagen, Morris,…: NN force at 3rd-order with Δ isobars, *PRC* (2018)

- **Plus: 2NF & 3NF with Bayesian uncertainties in LECs and EFT truncation errors** [e.g., P. Reinert et al., EPJA (2018); S. Wesolowski et al., *JPG* (2019); C. Drischler et al., *PRL* (2020); Volkotrub et al., *JPG* (2020); …]

- **Much progress, but work still needs to be done for a comprehensive account of all sources of uncertainty**

Microscopic modeling: many-body perturbation theory (MBPT)

$$E^{(1)} = \frac{1}{2}\sum_{12} n_1 n_2 \langle 12|(\overline{V}_{NN} + \overline{V}_{NN}^{\mathrm{med}}/3)|12\rangle,$$

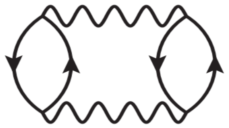

$$E^{(2)} = -\frac{1}{4}\sum_{1234} |\langle 12|\overline{V}_{\mathrm{eff}}|34\rangle|^2 \frac{n_1 n_2 \bar{n}_3 \bar{n}_4}{e_3 + e_4 - e_1 - e_2},$$

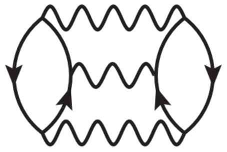

$$E^{(3)}_{\mathrm{pp}} = \frac{1}{8}\sum_{123456} \langle 12|\overline{V}_{\mathrm{eff}}|34\rangle\langle 34|\overline{V}_{\mathrm{eff}}|56\rangle\langle 56|\overline{V}_{\mathrm{eff}}|12\rangle \times \frac{n_1 n_2 \bar{n}_3 \bar{n}_4 \bar{n}_5 \bar{n}_6}{(e_3 + e_4 - e_1 - e_2)(e_5 + e_6 - e_1 - e_2)},$$

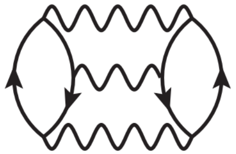

$$E^{(3)}_{\mathrm{hh}} = \frac{1}{8}\sum_{123456} \langle 12|\overline{V}_{\mathrm{eff}}|34\rangle\langle 34|\overline{V}_{\mathrm{eff}}|56\rangle\langle 56|\overline{V}_{\mathrm{eff}}|12\rangle \times \frac{\bar{n}_1 \bar{n}_2 n_3 n_4 n_5 n_6}{(e_1 + e_2 - e_3 - e_4)(e_1 + e_2 - e_5 - e_6)},$$

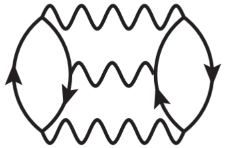

$$E^{(3)}_{\mathrm{ph}} = -\sum_{123456} \langle 12|\overline{V}_{\mathrm{eff}}|34\rangle\langle 54|\overline{V}_{\mathrm{eff}}|16\rangle\langle 36|\overline{V}_{\mathrm{eff}}|52\rangle \times \frac{n_1 n_2 \bar{n}_3 \bar{n}_4 n_5 \bar{n}_6}{(e_3 + e_4 - e_1 - e_2)(e_3 + e_6 - e_2 - e_5)},$$

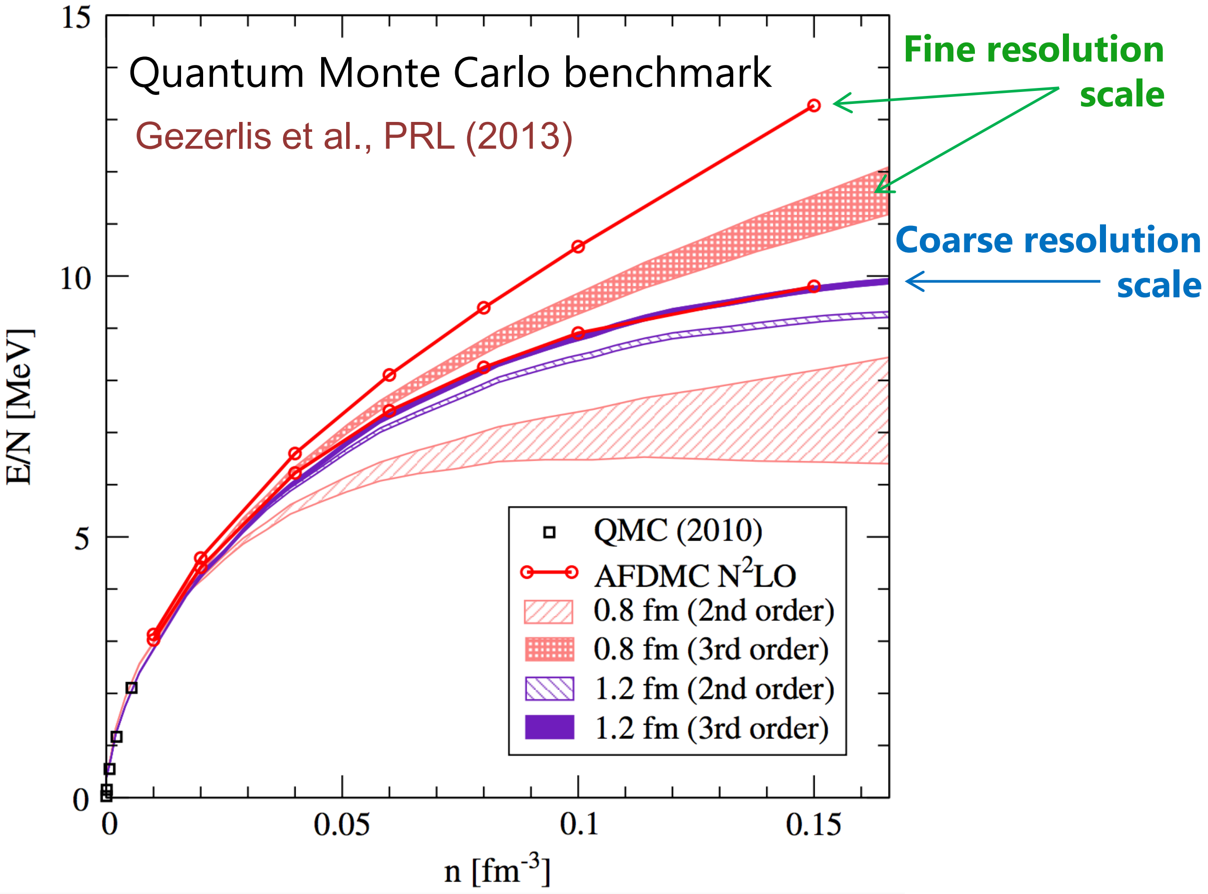

- 4^{th}-order MBPT diagrams up to N3LO in ChEFT [Drischler, Hebeler & Schwenk (2019)]
- Plus: EOS at finite temperature, arbitrary isospin asymmetry, response functions, single-particle potentials,…

Uncertainties in symmetric nuclear matter equation of state

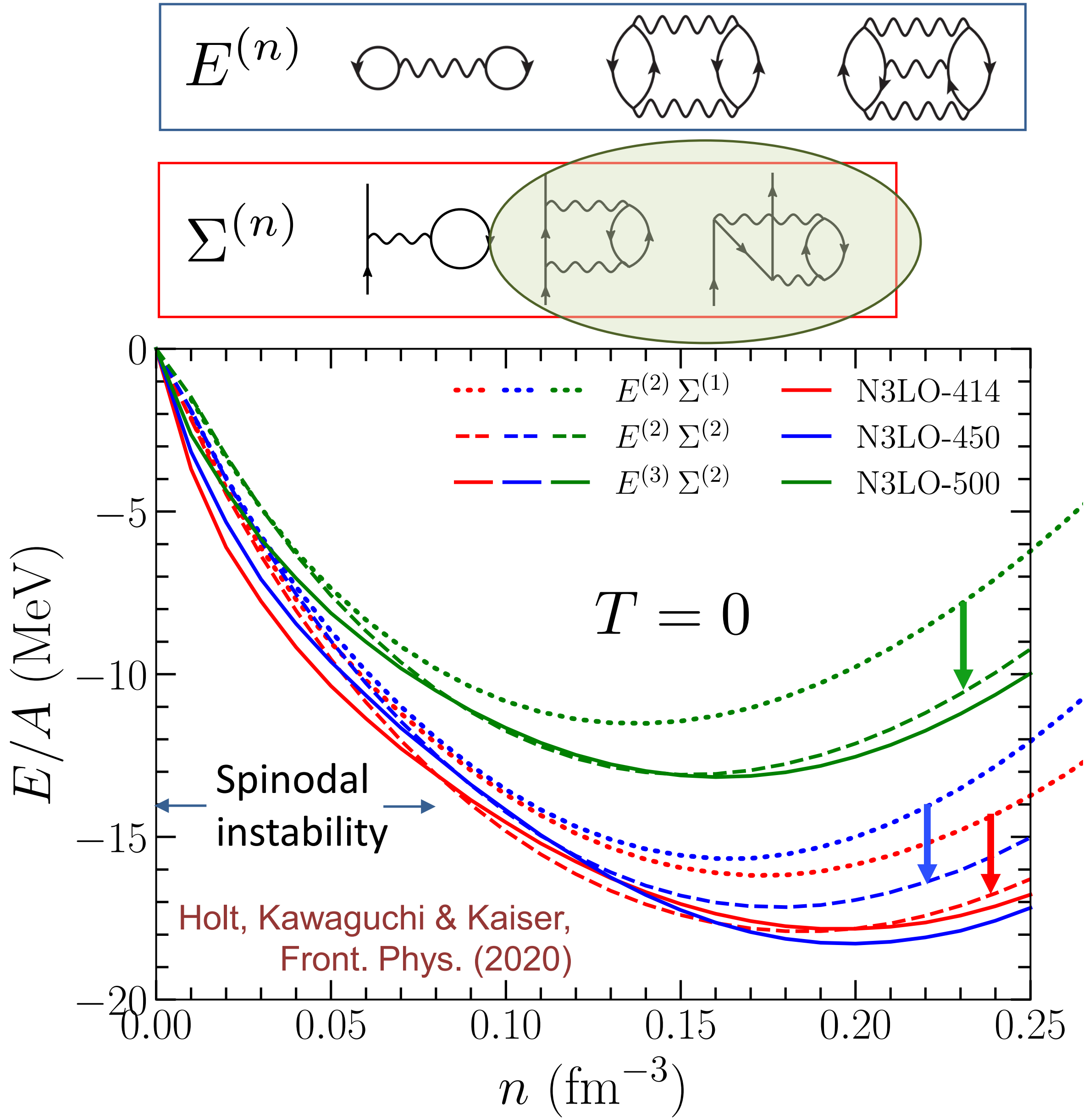

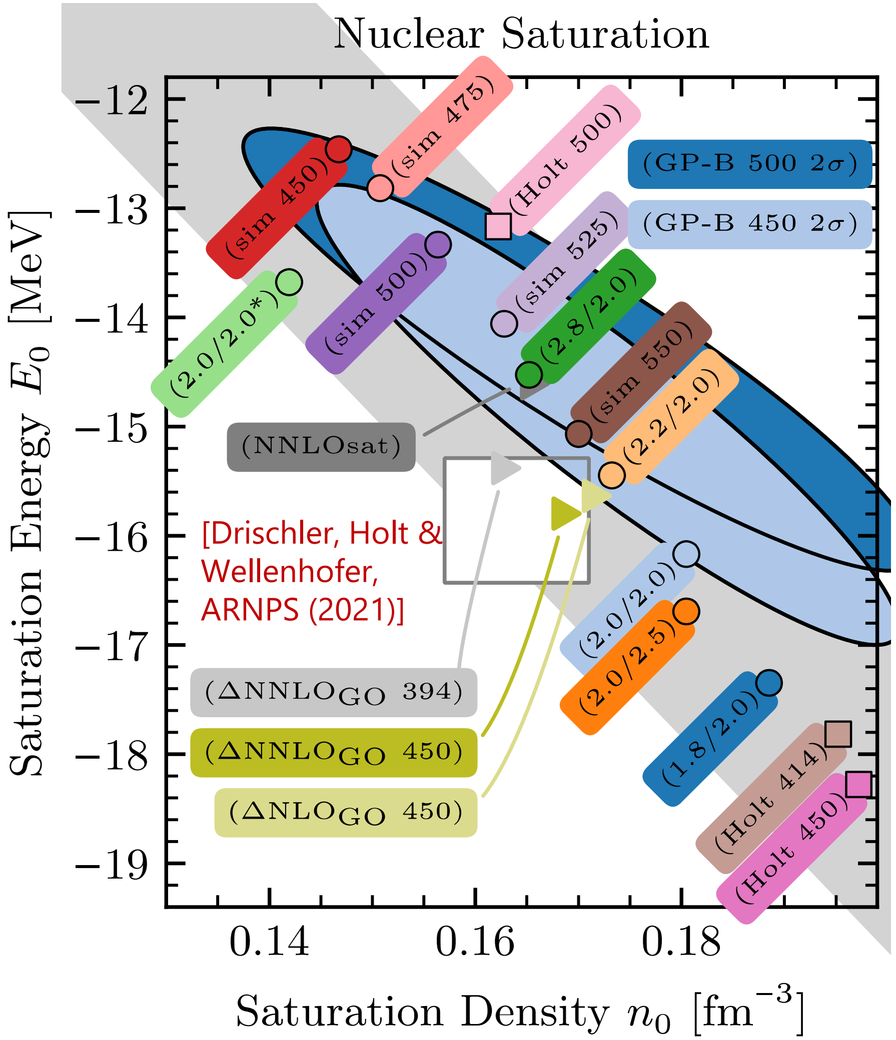

- **Saturation point is a fine-tuned quantity**

Uncertainties in pure neutron matter equation of state

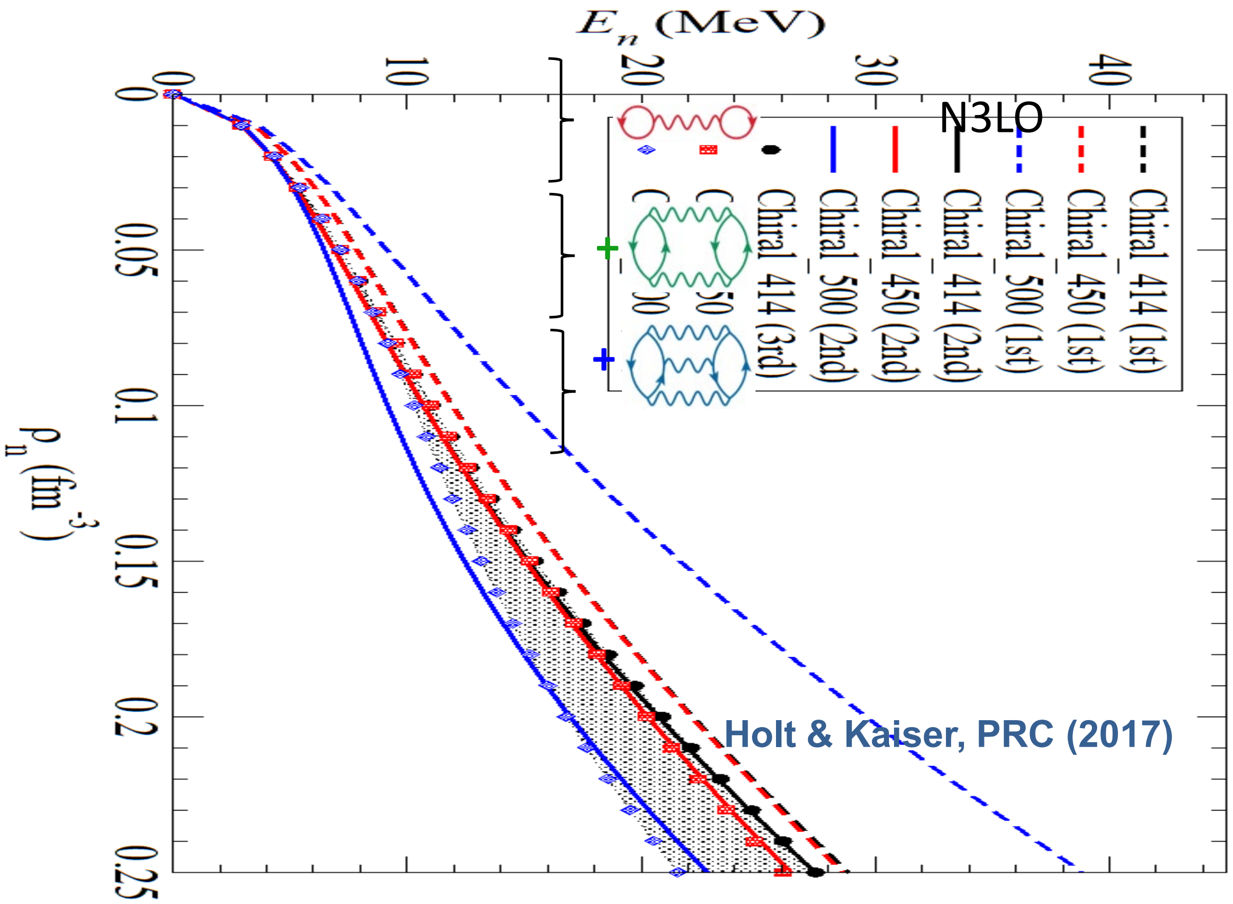

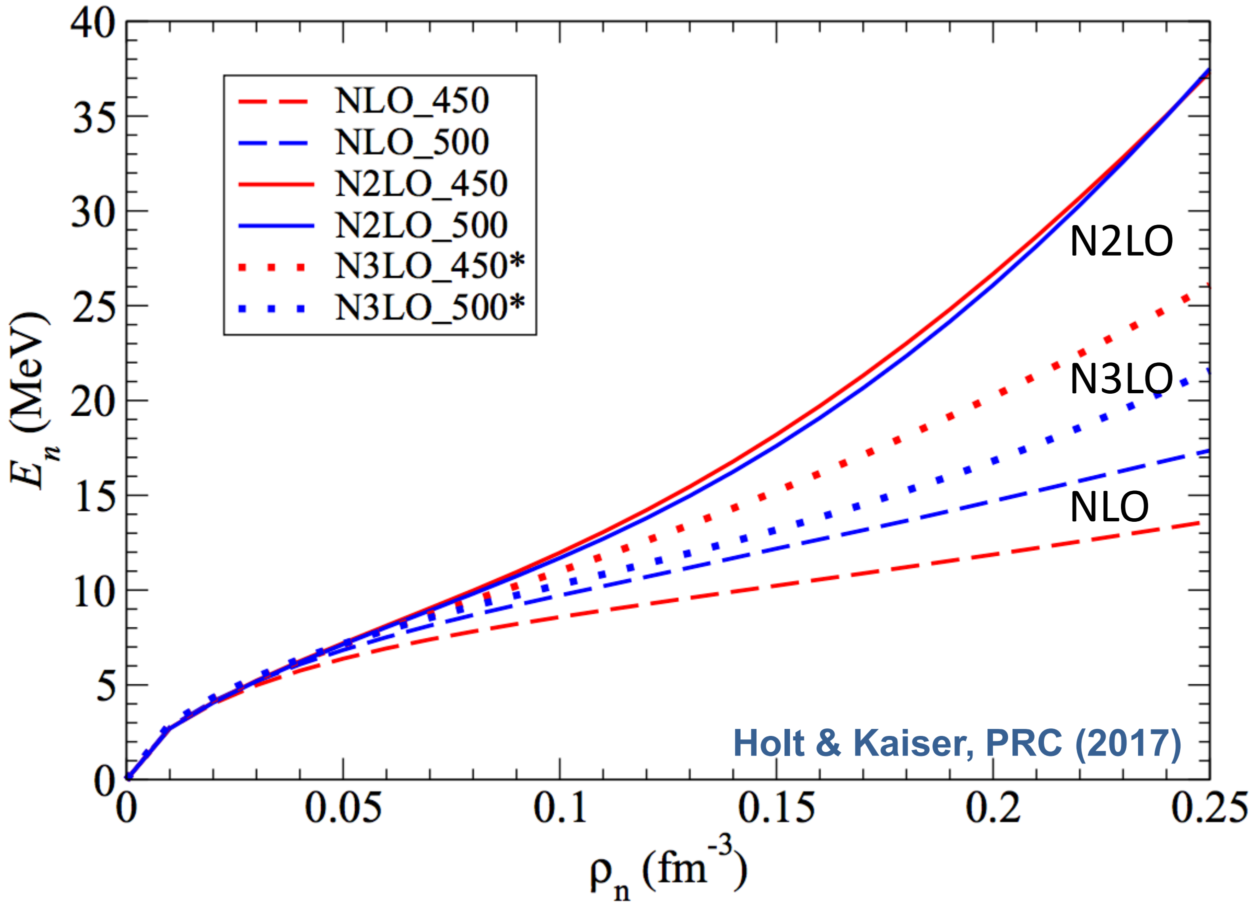

Sources of uncertainty:

- Scale dependence
- Convergence in many-body perturbation theory
- Convergence in chiral expansion largest uncertainty

Combined EOS constraints from theory and experiment

- Construct some EOS model with parameters $\vec{a}$ $\frac{E}{A}(\rho, \delta = 0) = \frac{3k_F^2}{10m} + \frac{k_F^3}{9\pi^2}\left(a_0 + a_1\,\beta + \frac{1}{2}a_2\,\beta^2 + \frac{1}{6}a_3\,\beta^3\right)$

$$\beta = \frac{k_F - k_r}{k_r}$$

- Bayes' Theorem: $P(\vec{a}|data) \sim P(data|\vec{a})P(\vec{a})$

Posterior

Likelihood of data given a probability distribution for $\vec{a}$

Beliefs about parameters $\vec{a}$ before measurements

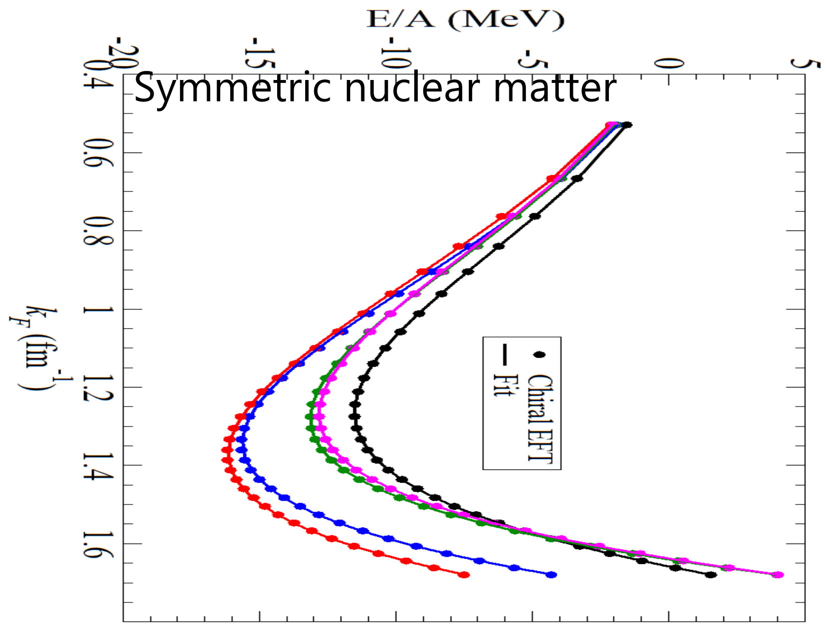

- Strategy:
  1. Find useful parametrization for the equation of state
  2. Obtain priors from **chiral EFT predictions**
  3. Use laboratory measurements of finite nuclei (saturation binding energy and density, incompressibility, symmetry energy,…) to obtain likelihood functions and posteriors

Prior and posterior EOS distributions

- Order in the chiral expansion
- Scale dependence of nuclear force
- Quantum many-body method

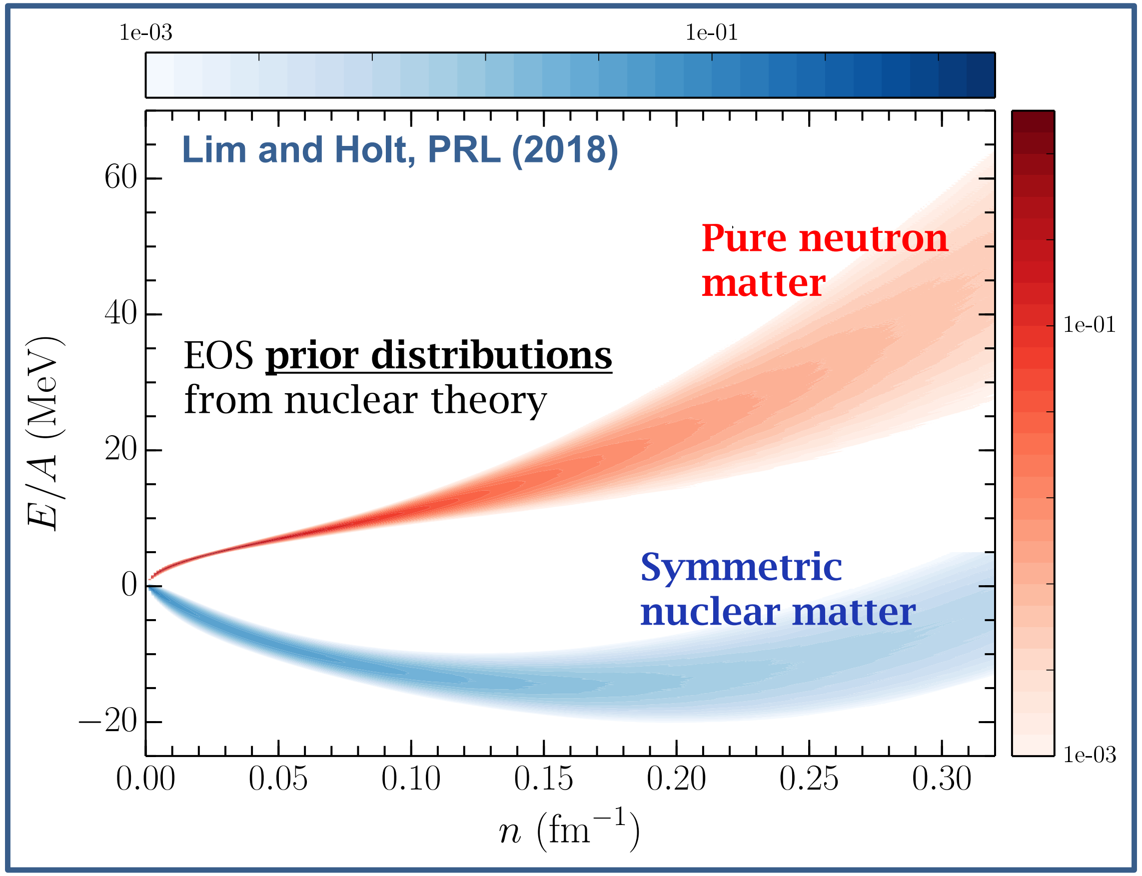

- Nuclear binding energies
- Experimental constraints on isospin-asymmetry energy

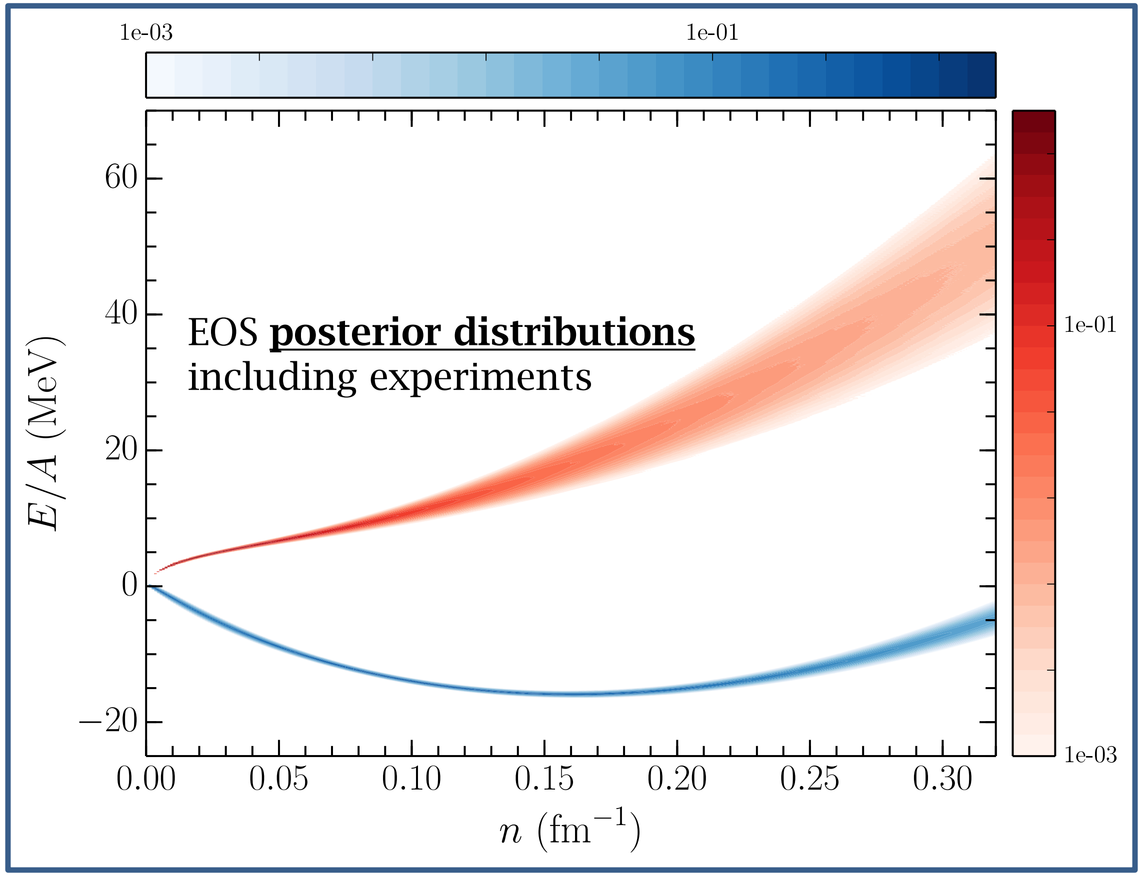

Microscopic modeling: many-body perturbation theory (MBPT)

Drischler, Holt & Wellenhofer, ARNPS (2021)

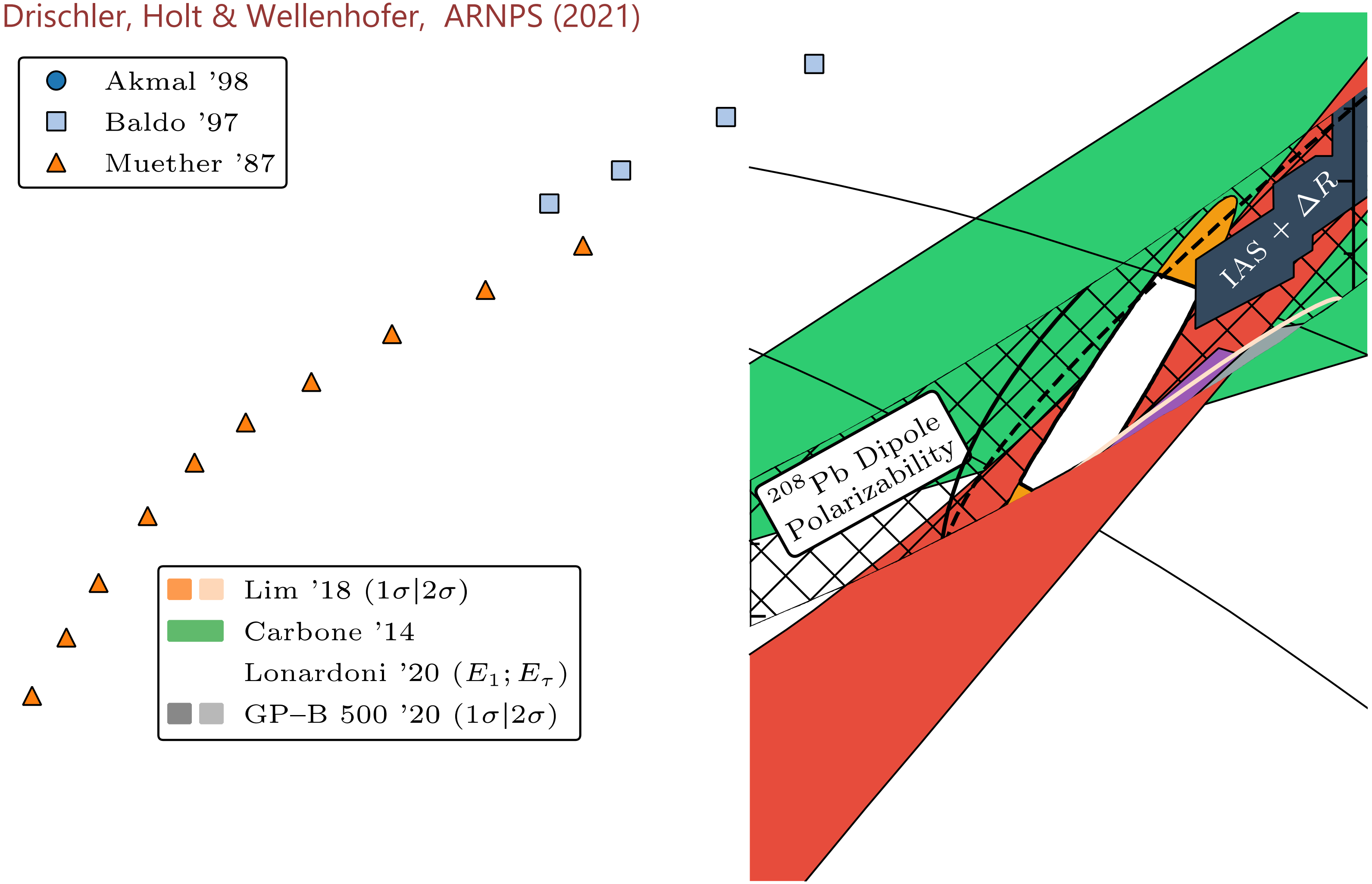

Derived mass-radius relation

Lim and Holt, PRL (2018)

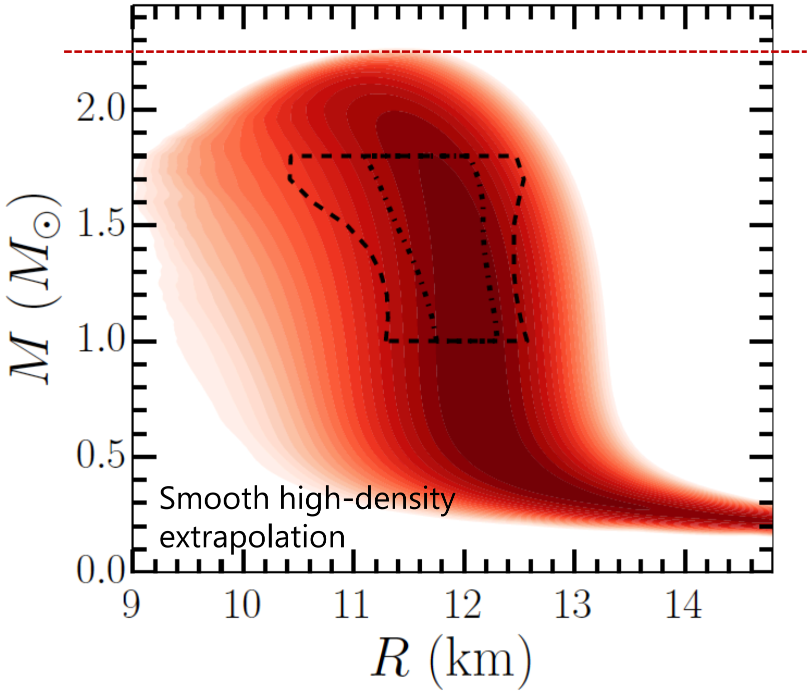

- $10.4\,\mathrm{km} < R_{1.4} < 12.8\,\mathrm{km}$
- $140 < \Lambda_{1.4} < 520$
- $M_{\max} \simeq 2.25\, M_\odot$

Abbott et al., PRL (2018)

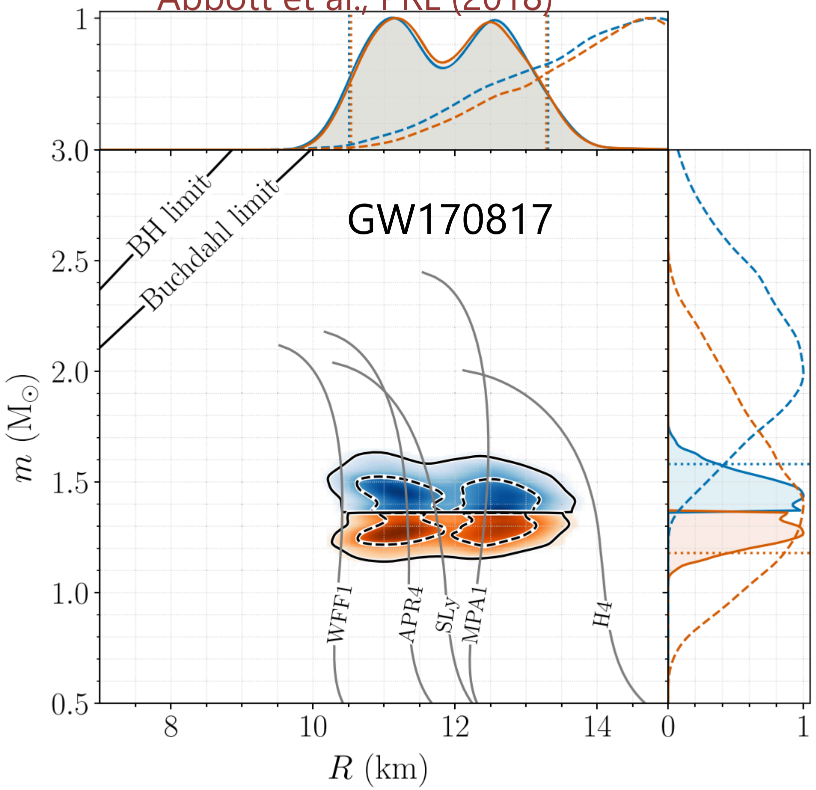

- $10.7\,\mathrm{km} \lesssim R_{1.4} \lesssim 13.6\,\mathrm{km}$
- $70 < \Lambda_{1.4} < 580$
- $M_{\max} \simeq 2.2 - 2.3\, M_\odot$

Tews, Margueron & Reddy, PRC (2018)

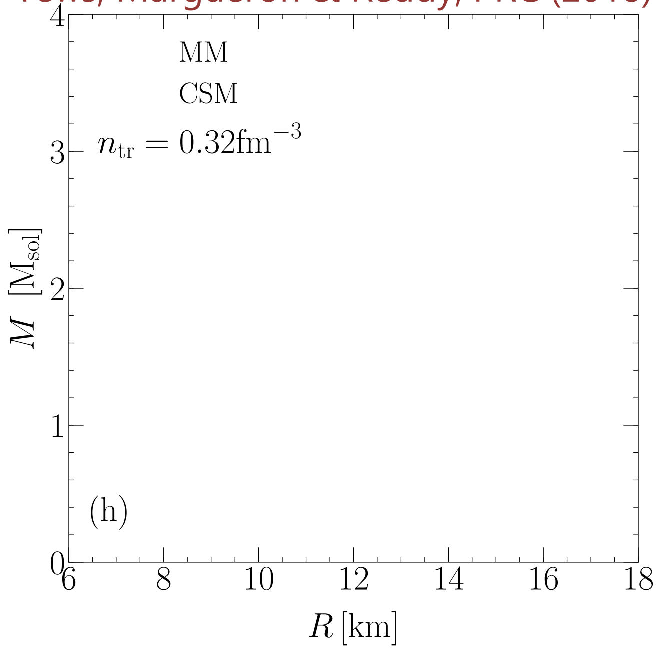

- Choice of transition density has strong effect on EOS inference

Propagated uncertainties

[Drischler, Holt & Wellenhofer, ARNPS (2021)]

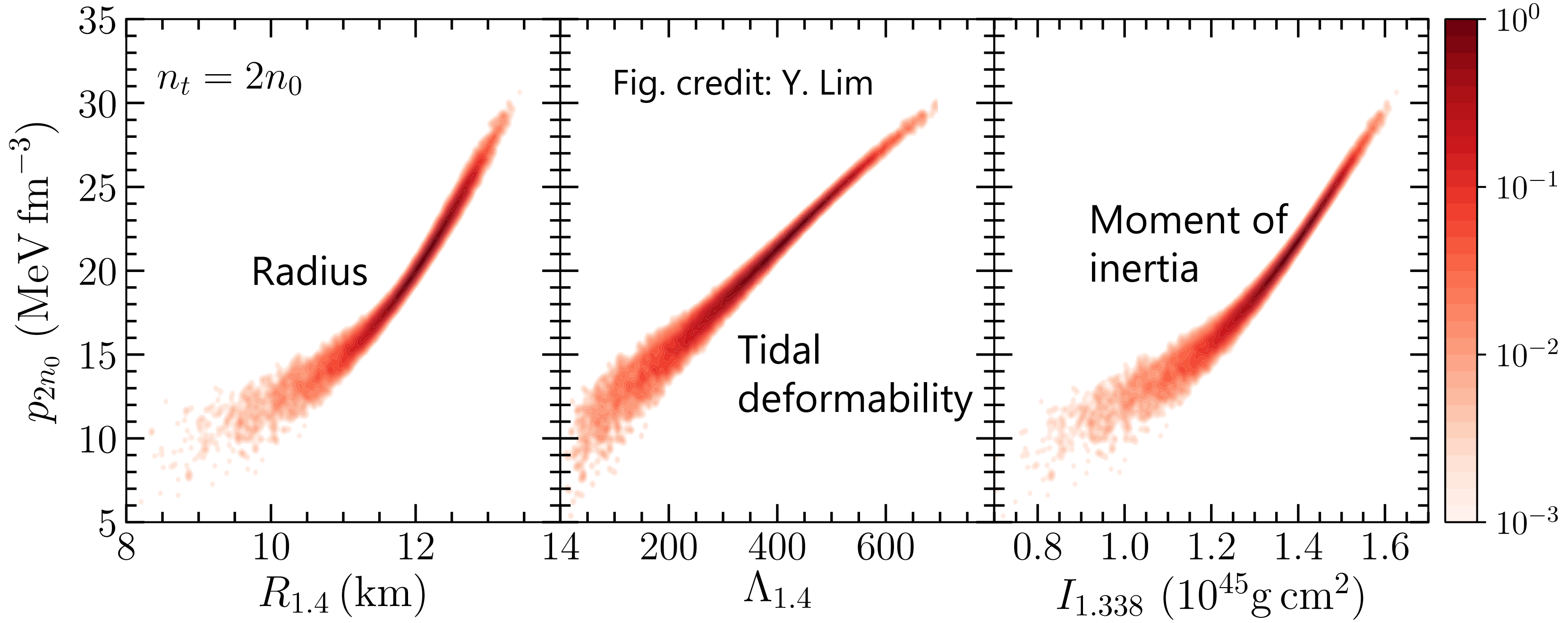

S. K. Greif et al., ApJ (2020)

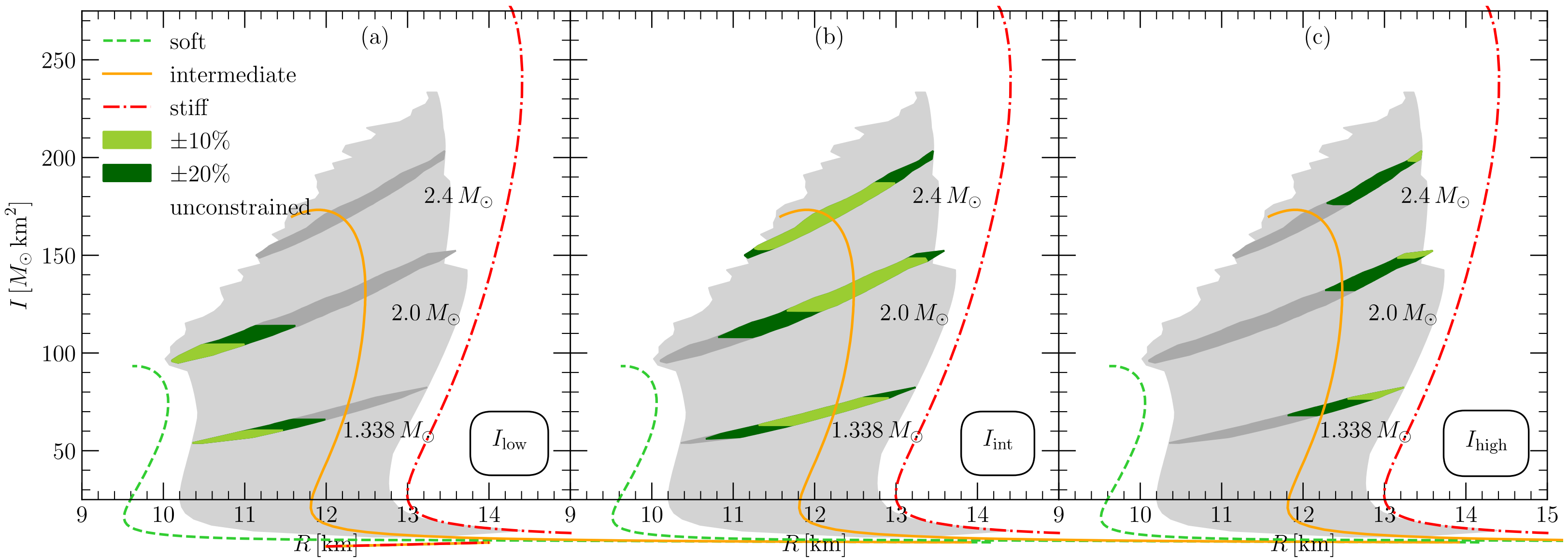

^{208}Pb neutron skin thickness from experiment and theory

$$\mathrm{PREX-II:}\;\; R_{\mathrm{skin}}(^{208}\mathrm{Pb}) = 0.283 \pm 0.071\,\mathrm{fm}$$

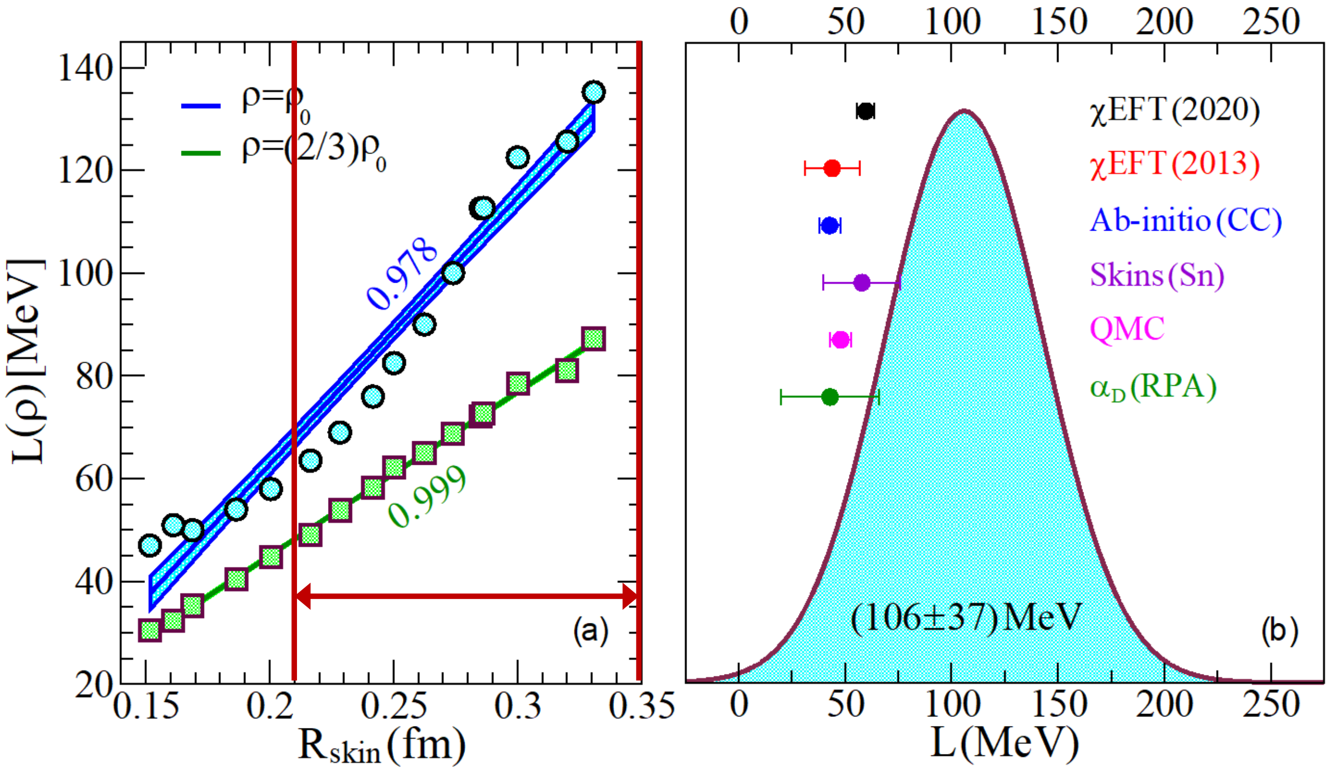

B. R. Reed et al., PRL (2021)

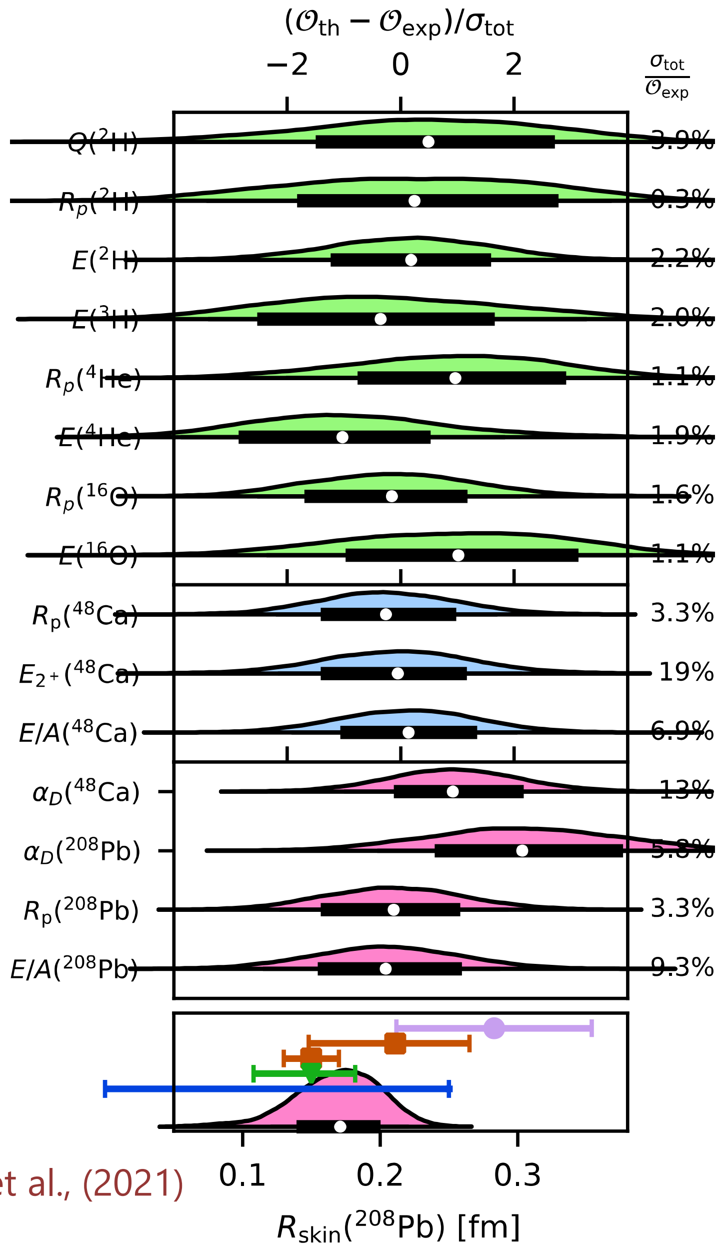

B. Hu et al., (2021)

Combined theory, experiment, and observational constraints

Smooth high-density extrapolation

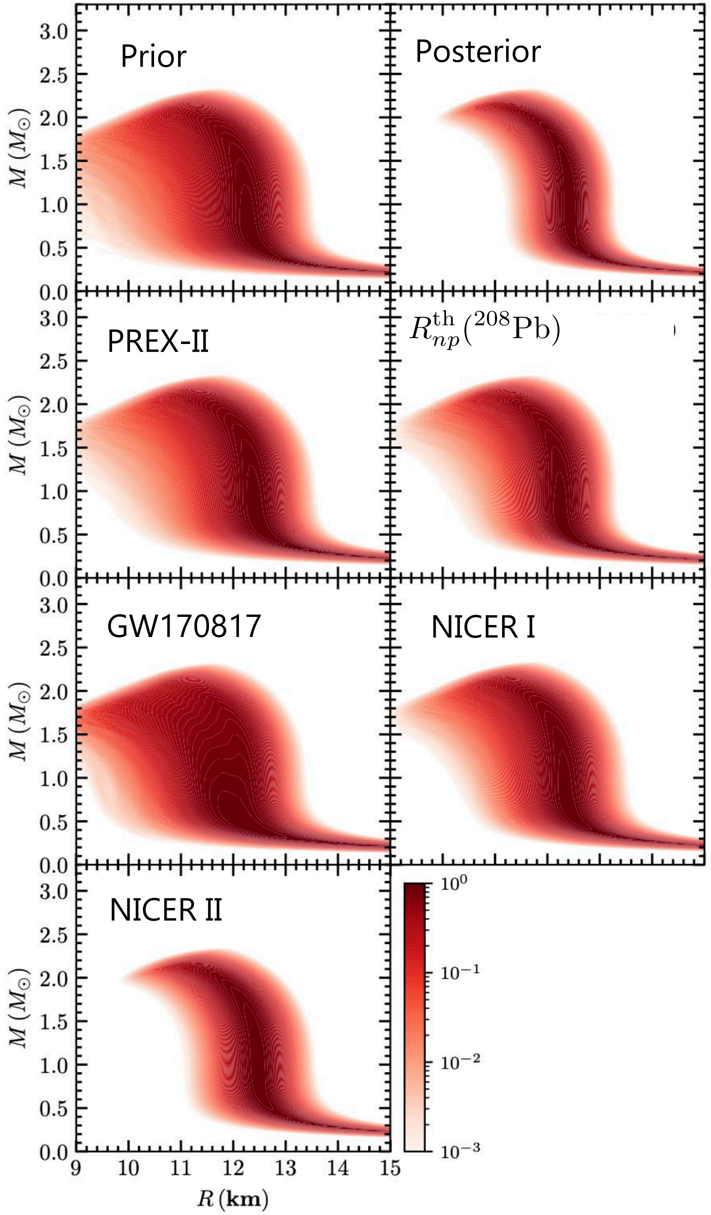

Maximally-stiff high-density extrapolation

Transition density varied from $2-4n_0$

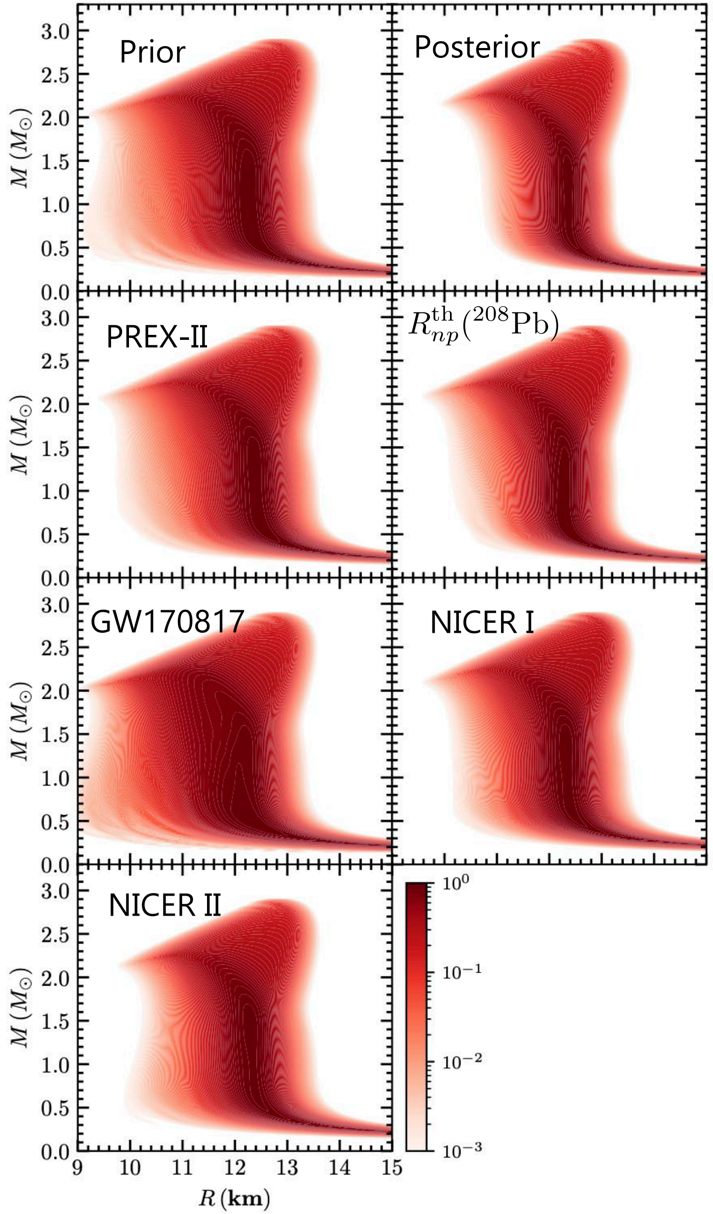

Posteriors for $R_{1.4}$

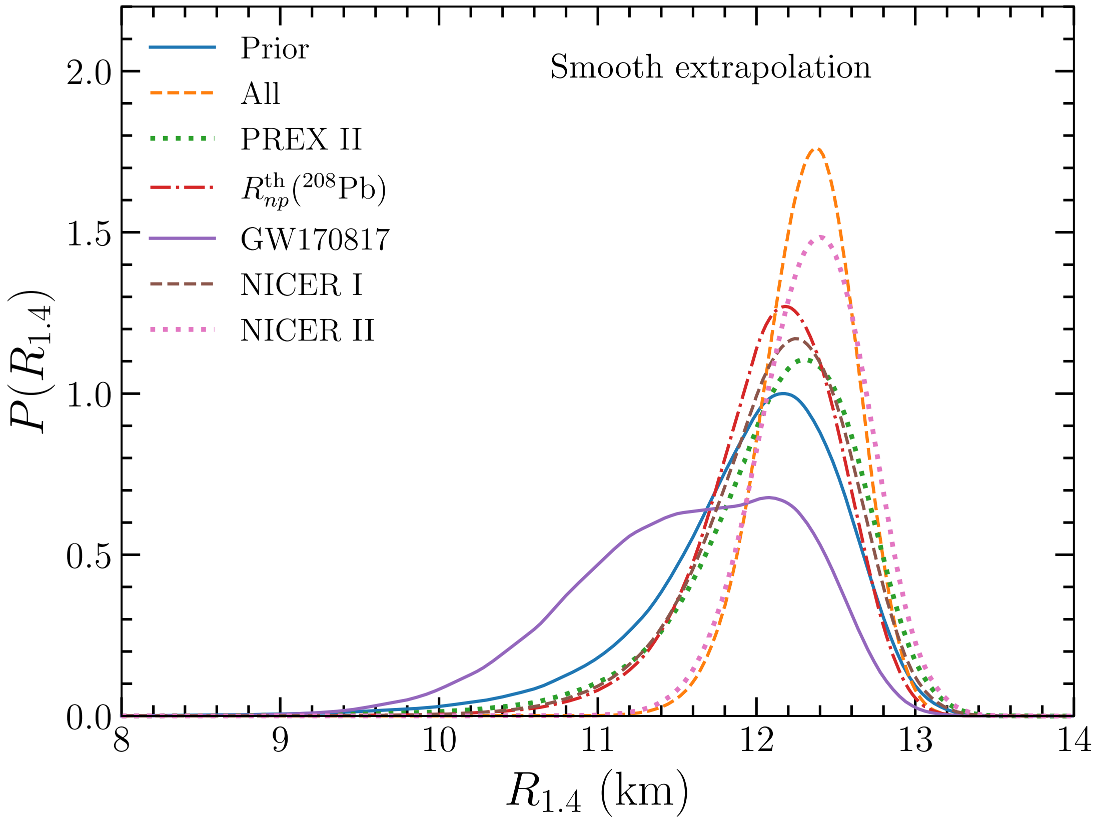

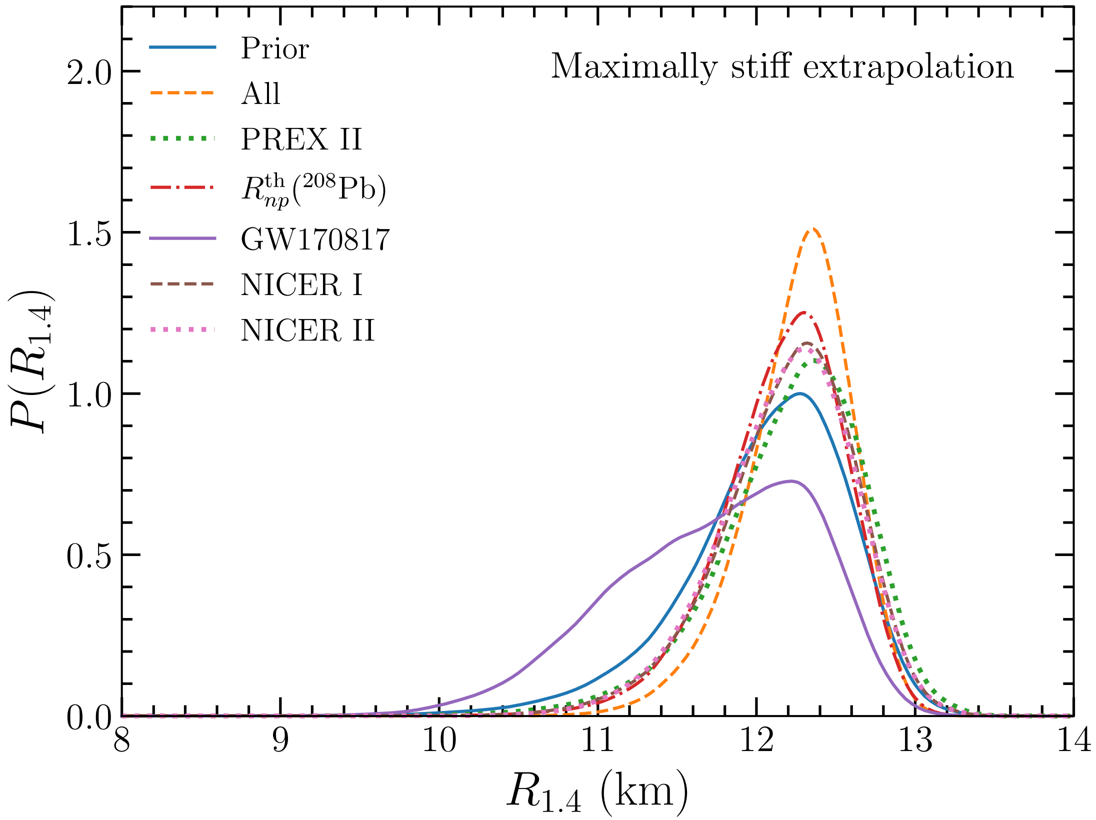

$$R_{1.4}(\text{Prior}) = 12.16^{+0.59}_{-1.42}\,\text{km}\,(90\%)$$

$$R_{1.4}(\text{Posterior}) = 12.38^{+0.39}_{-0.57}\,\text{km}\,(90\%)$$

$$R_{1.4}(\text{Prior}) = 12.28^{+0.49}_{-1.20}\,\text{km}\,(90\%)$$

$$R_{1.4}(\text{Posterior}) = 12.36^{+0.38}_{-0.73}\,\text{km}\,(90\%)$$

Posteriors for $R_{2.0}$

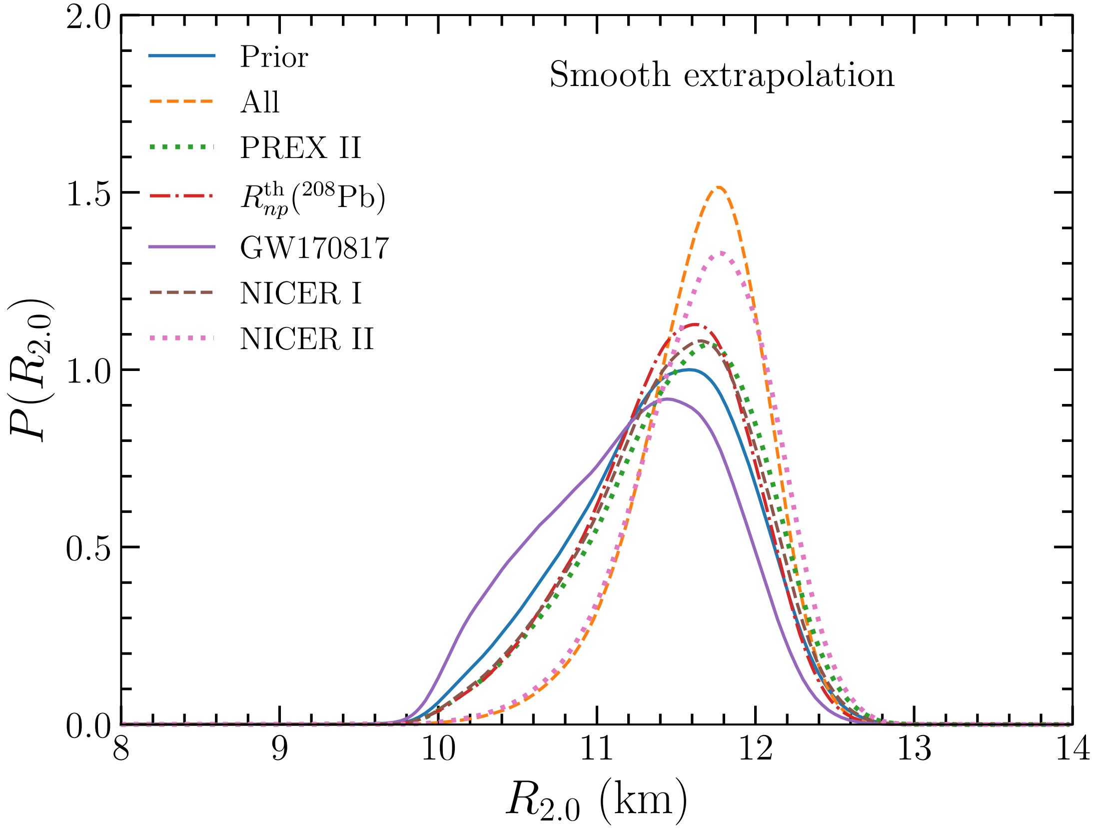

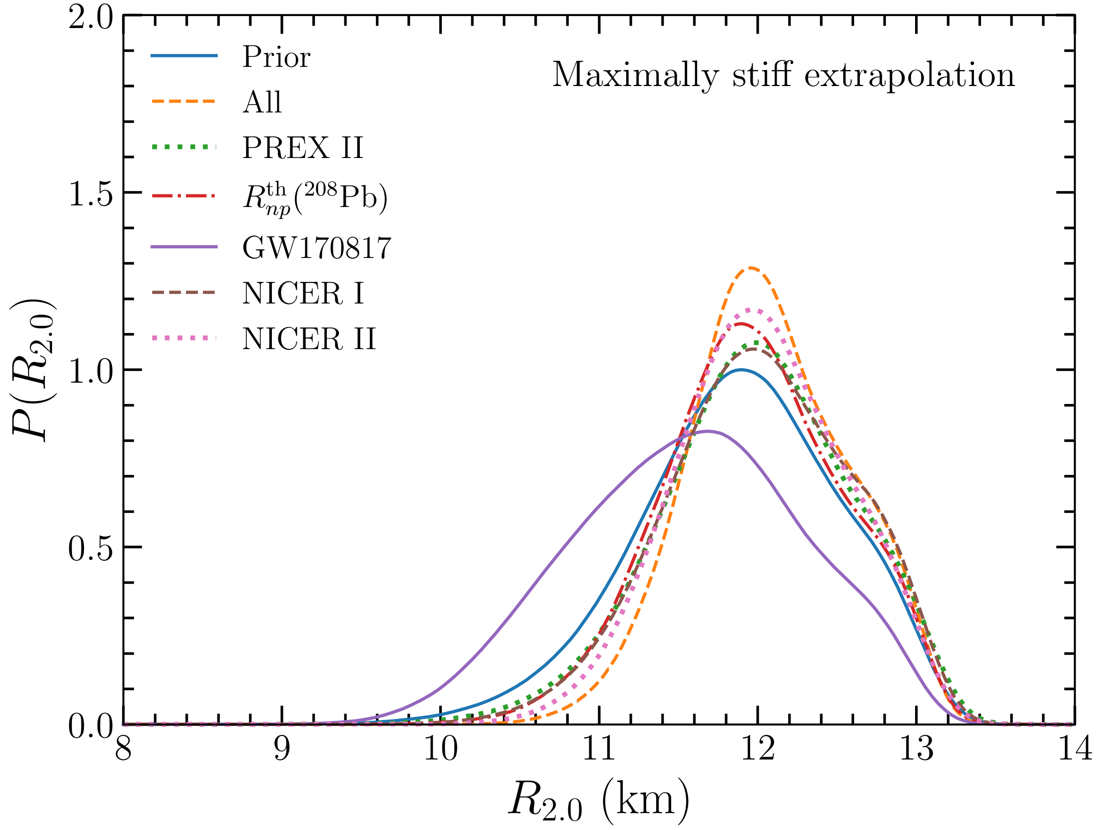

$$R_{2.0}(\text{Prior}) = 11.58^{+0.61}_{-1.19}\,\text{km}\,(90\%)$$

$$R_{2.0}(\text{Posterior}) = 11.76^{+0.46}_{-0.84}\,\text{km}\,(90\%)$$

$$R_{2.0}(\text{Prior}) = 11.90^{+0.97}_{-1.15}\,\text{km}\,(90\%)$$

$$R_{2.0}(\text{Posterior}) = 11.96^{+0.94}_{-0.71}\,\text{km}\,(90\%)$$

Posteriors for $\Lambda_{1.4}$

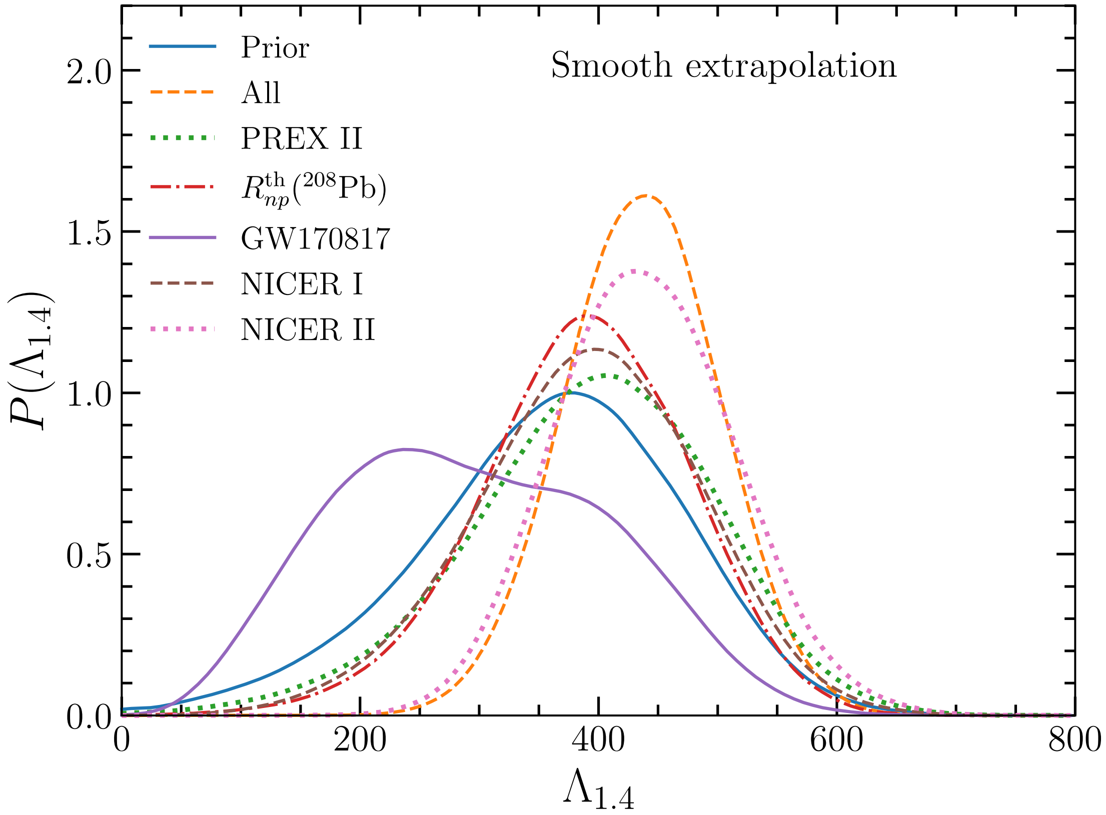

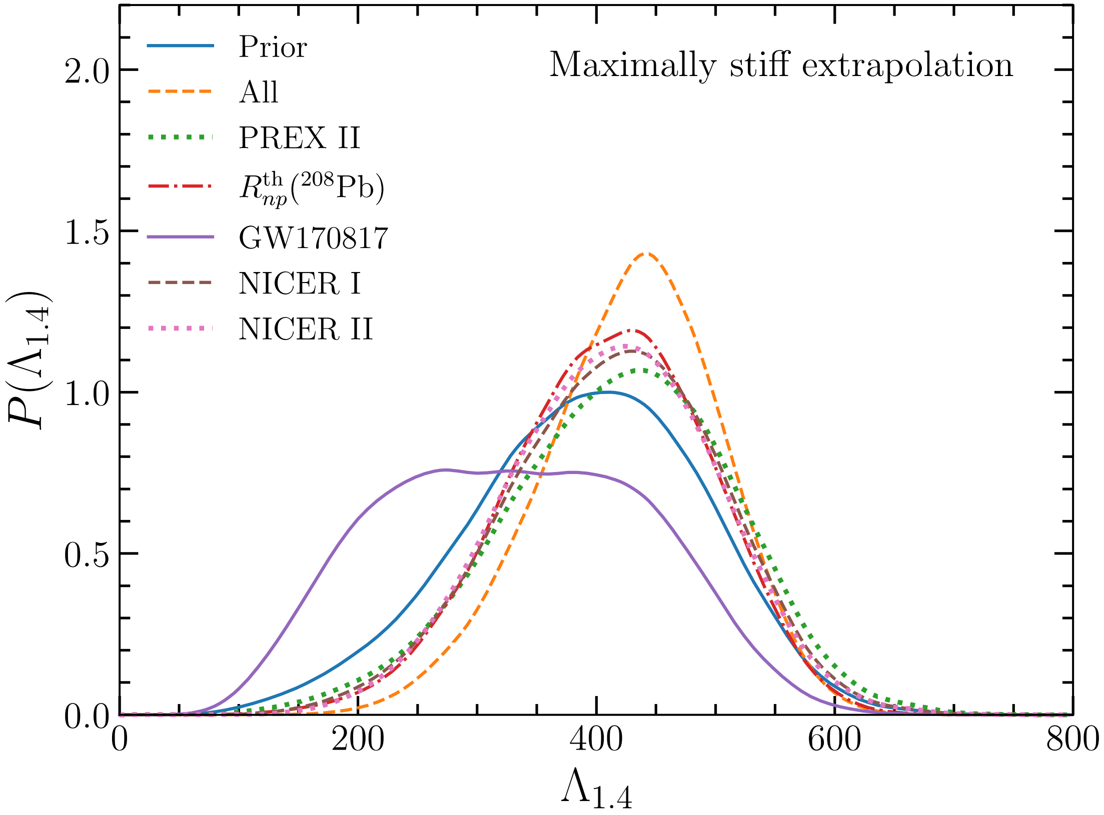

$$\Lambda_{1.4}(\text{Prior}) = 376^{+151}_{-216}\ (90\%)$$

$$\Lambda_{1.4}(\text{Posterior}) = 440^{+101}_{-113}\ (90\%)$$

$$\Lambda_{1.4}(\text{Prior}) = 408^{+136}_{-195}\ (90\%)$$

$$\Lambda_{1.4}(\text{Posterior}) = 440^{+103}_{-144}\ (90\%)$$

Posteriors for $I_{1.338}$

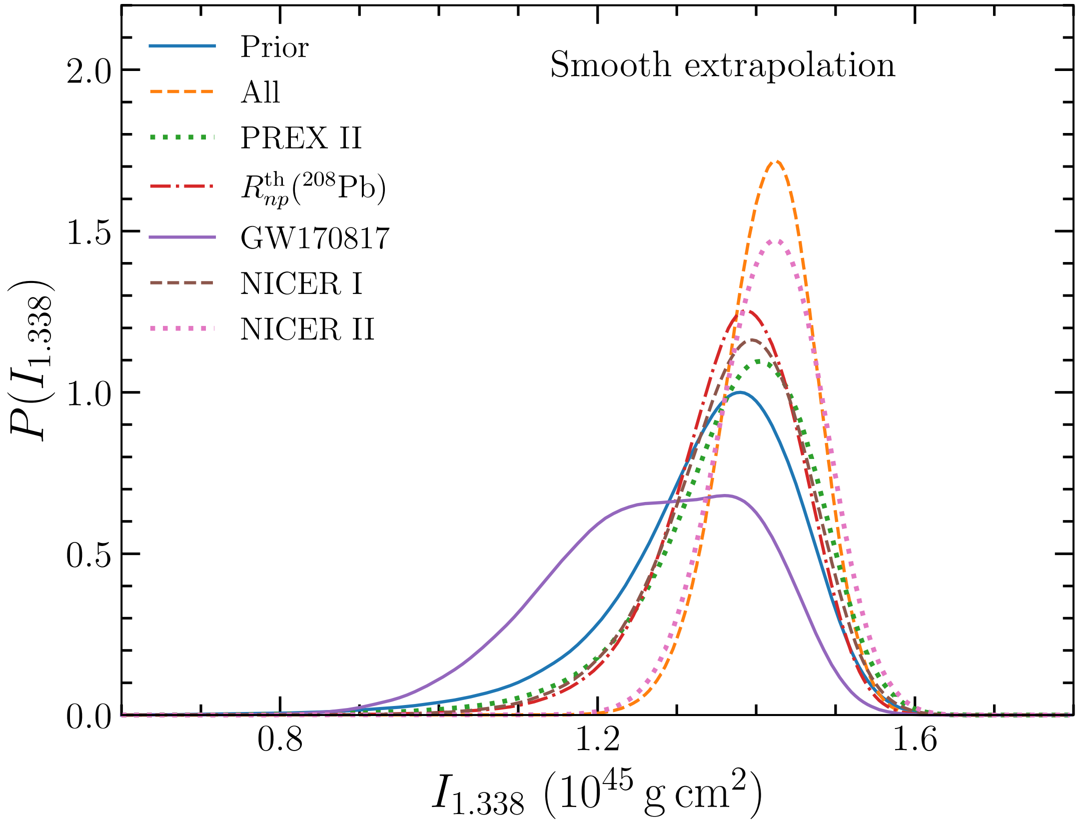

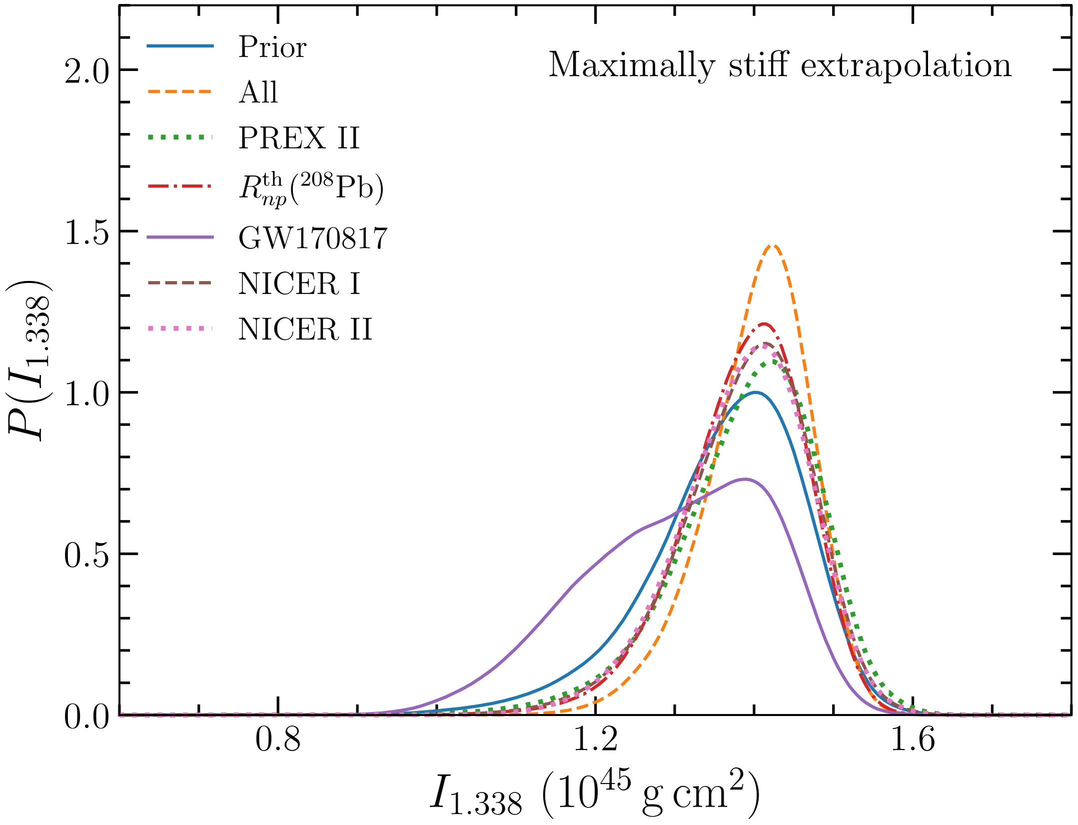

$$I_{1.338}({\rm Prior}) = 1.38^{+0.12}_{-0.26} \times 10^{45}\,{\rm g\,cm^2}(90\%)$$

$$I_{1.338}({\rm Posterior}) = 1.43^{+0.07}_{-0.12} \times 10^{45}\,{\rm g\,cm^2}(90\%)$$

$$I_{1.338}({\rm Prior}) = 1.40^{+0.10}_{-0.22} \times 10^{45}\,{\rm g\,cm^2}(90\%)$$

$$I_{1.338}({\rm Posterior}) = 1.43^{+0.07}_{-0.15} \times 10^{45}\,{\rm g\,cm^2}(90\%)$$

Posteriors for $R_{1.4}$

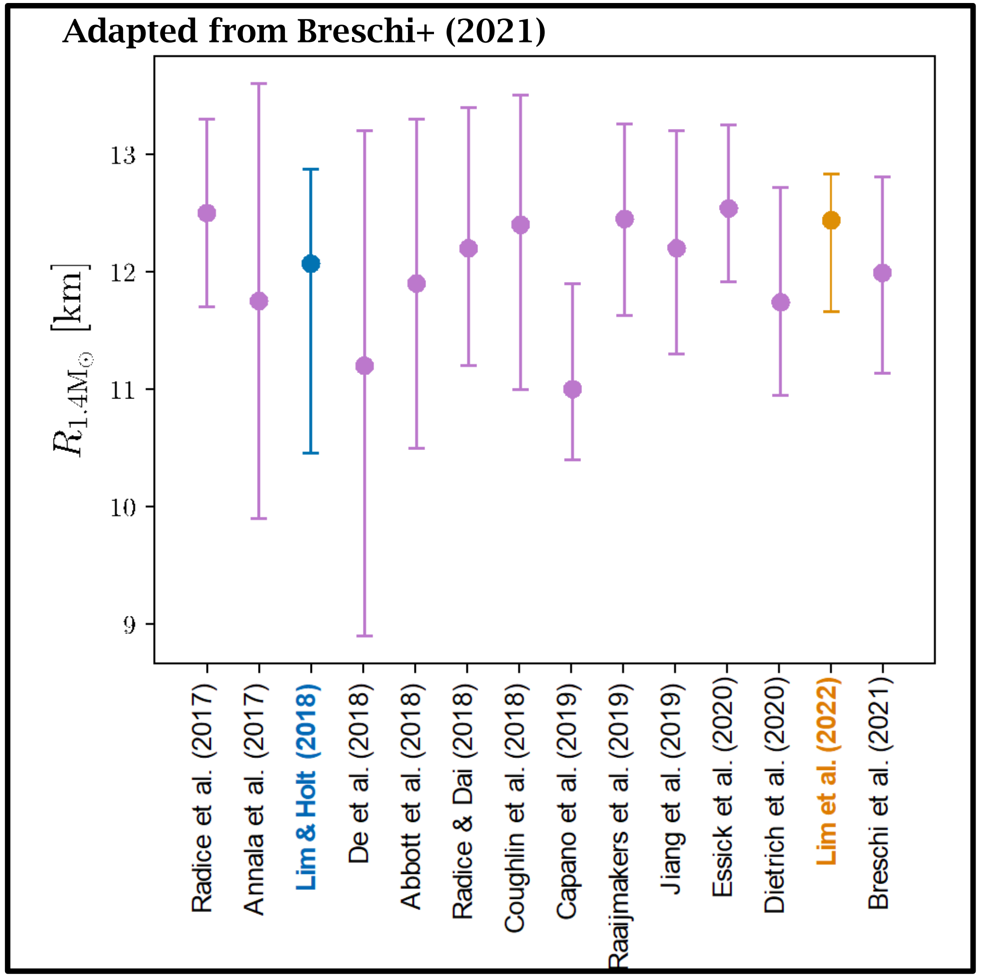

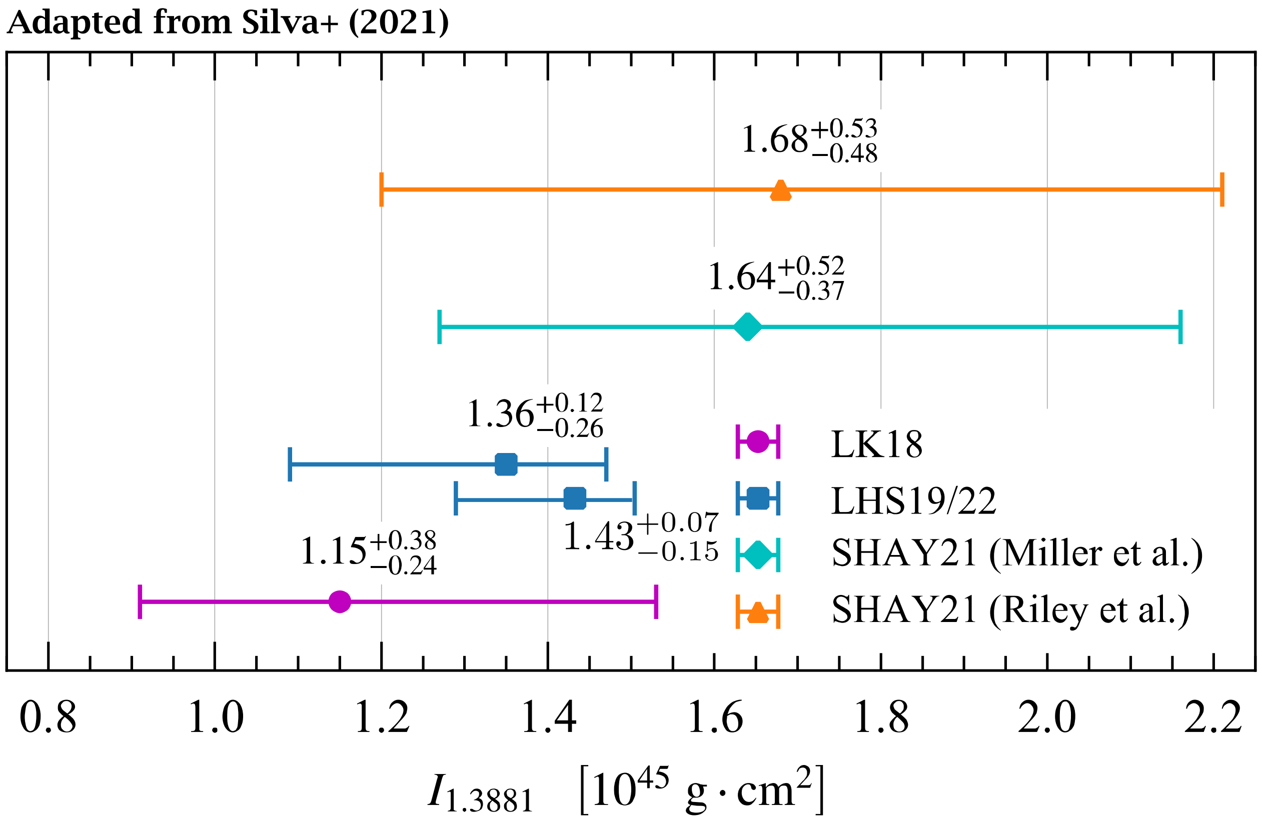

Neutron star radii from NICER and tidal deformabilities from LIGO/Virgo

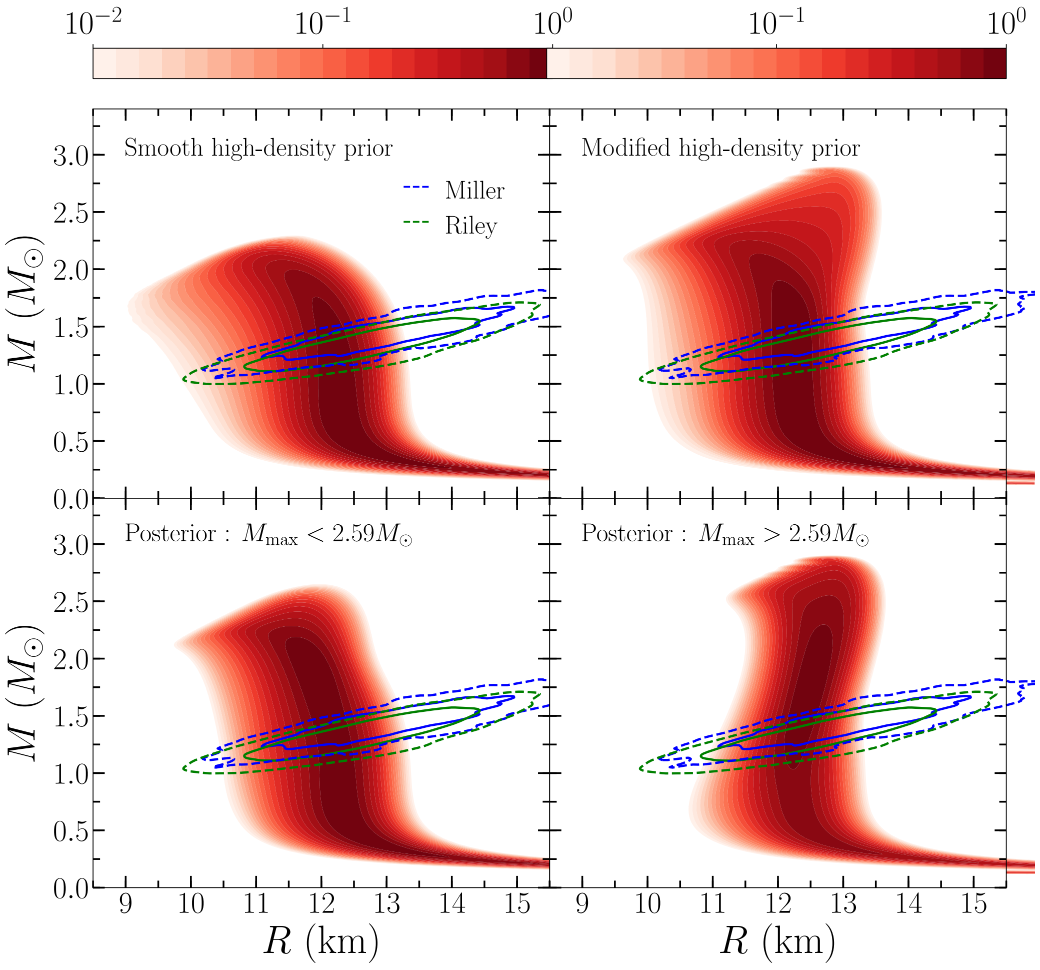

Lim, Bhattacharya, Holt & Pati, PRCL (2021)

Neutron star radii from NICER and tidal deformabilities from LIGO/Virgo

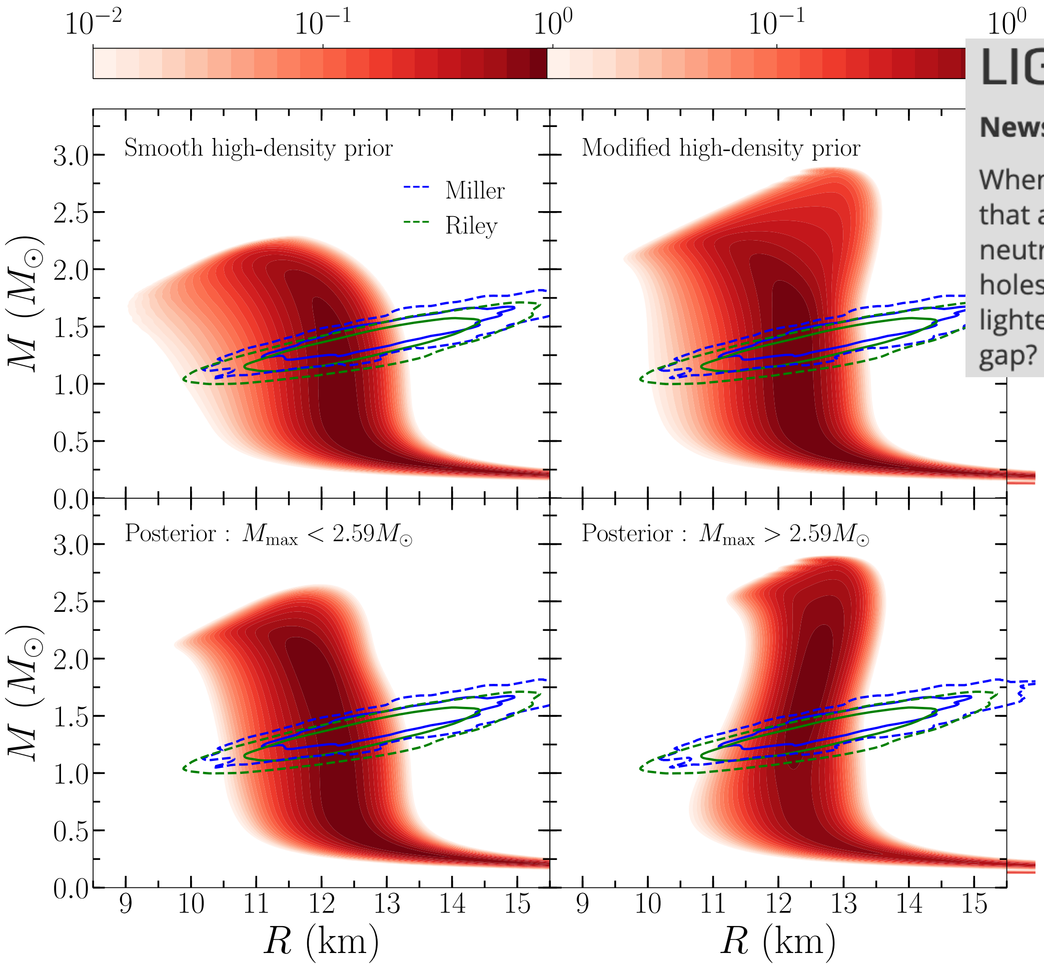

Lim, Bhattacharya, Holt & Pati, PRCL (2021)

$$M = 2.50 - 2.67\, M_\odot$$

LIGO-Virgo Finds Mystery Object in "Mass Gap"

News Release • June 23, 2020

When the most massive stars die, they collapse under their own gravity and leave behind black holes; when stars that are a bit less massive die, they explode in a supernova and leave behind dense, dead remnants of stars called neutron stars. For decades, astronomers have been puzzled by a gap that lies between neutron stars and black holes: the heaviest known neutron star is no more than 2.5 times the mass of our sun, or 2.5 solar masses, and the lightest known black hole is about 5 solar masses. The question remained: does anything lie in this so-called mass gap?

Neutron star radii from NICER and tidal deformabilities from LIGO/Virgo

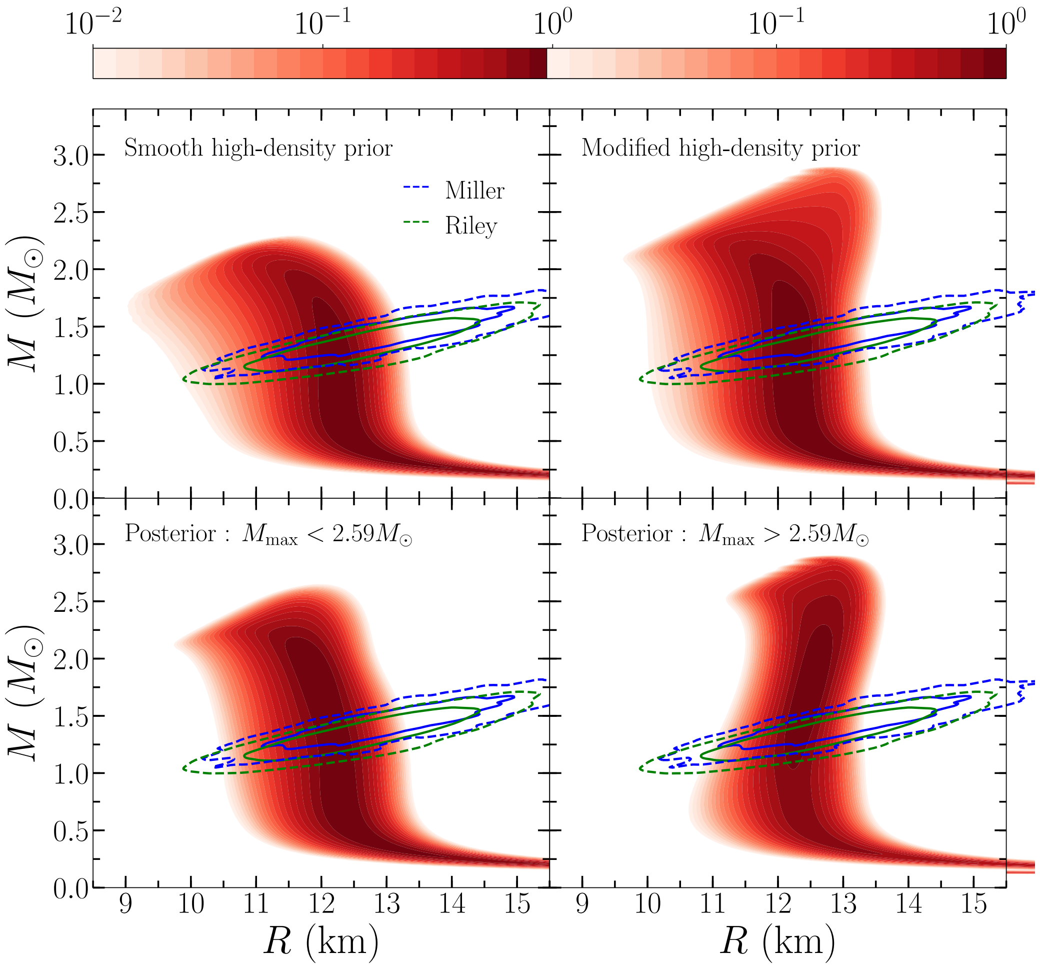

Lim, Bhattacharya, Holt & Pati, arXiv:2007.06526

Lim, Bhattacharya, Holt & Pati, PRCL (2021)

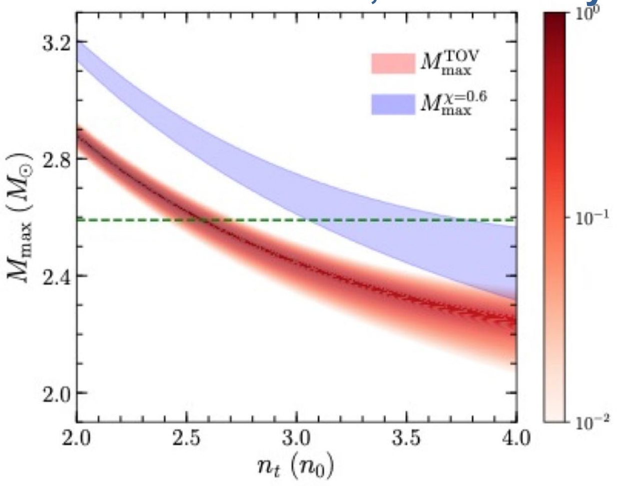

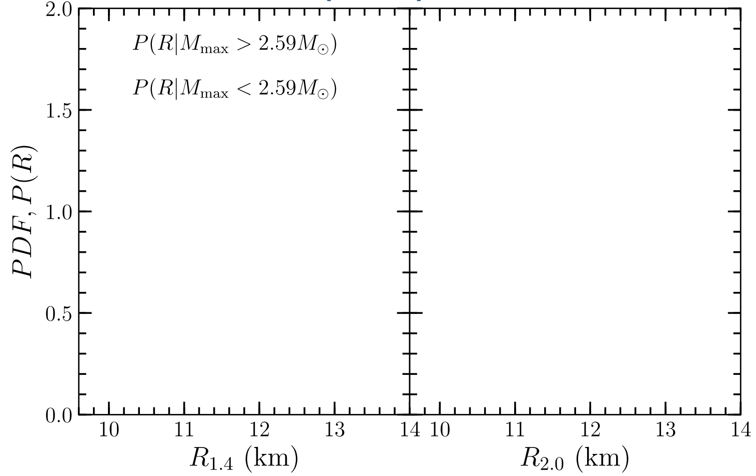

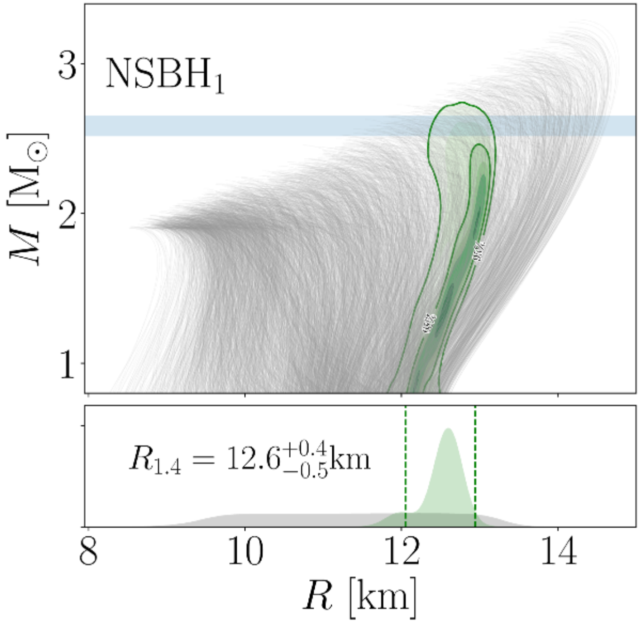

Tews et al., ApJL (2021)

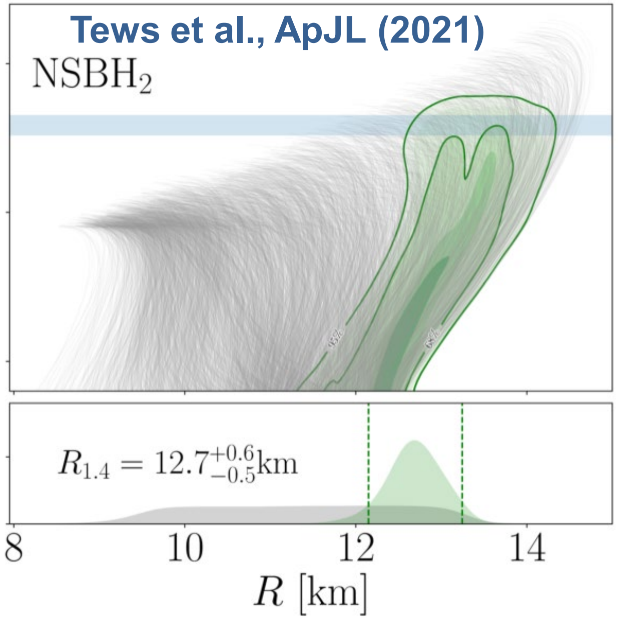

Summary and future directions

- New era of major observational campaigns to study the properties of neutron stars

- Complementary theoretical models with accurate nuclear physics inputs needed to guide and interpret observations

- All constraints from nuclear theory, nuclear experiment, and neutron star observations consistent without the need to adopt exotic high-density degrees of freedom

▷ **Comprehensive uncertainty analysis of chiral nuclear forces including variations in the resolution scale, 2N & 3N LECs, and EFT truncation errors**